Glyphosate Inhibits Melanization and Increases Susceptibility to Infection in Insects

Daniel F. Q. Smith[1], Emma Camacho[1], Raviraj Thakur[2†¶], Alexander J. Barron[3†], Yuemei Dong[1], George Dimopoulos[1], Nichole A. Broderick[3Ω], Arturo Casadevall[1Ω*]

[1]Department of Molecular Microbiology and Immunology, Johns Hopkins Bloomberg School of Public Health, [2] Department of Otolaryngology, Head and Neck Surgery, Johns Hopkins Medicine, Baltimore, MD 21205, [3] Department of Biology, Johns Hopkins University, Baltimore MD 21218, United States of America.

Running title: Glyphosate Inhibits Melanization in Insects

*Correspondence: acasade1@jhu.edu
† Authors contributed equally
Ω N.A.B. and A.C. share senior authorship
¶ Current Address: Cancer Early Detection Advanced Research Center, Knight Cancer Institute, Oregon Health and Science University, Portland, OR 97201

ABSTRACT

Melanin, a black-brown pigment found throughout all kingdoms of life, has diverse biological functions including: UV protection, thermoregulation, oxidant scavenging, arthropod immunity, and microbial virulence. Given melanin's broad roles in the biosphere, particularly in insect immune defenses, it is important to understand how exposure to ubiquitous environmental contaminants affects melanization. Glyphosate – the most widely used herbicide globally – inhibits melanin production, which could have wide-ranging implications in the health of many organisms, including insects. Here, we demonstrate that glyphosate has deleterious effects on insect health in two evolutionary distant species, *Galleria mellonella* (Lepidoptera: Pyralidae) and *Anopheles gambiae* (Diptera: Culicidae), suggesting a broad effect in insects. Glyphosate reduced survival of *G. mellonella* caterpillars following infection with the fungus *Cryptococcus neoformans* and decreased the size of melanized nodules formed in hemolymph, which normally help eliminate infection. Glyphosate also increased the burden of the malaria-causing parasite *Plasmodium falciparum* in *A. gambiae* mosquitoes, altered uninfected mosquito survival, and perturbed the microbial composition of adult mosquito midguts. Our results show that glyphosate's mechanism of melanin inhibition involves antioxidant synergy and disruption of the reaction oxidation-reduction balance Overall, these findings suggest that glyphosate's environmental accumulation could render insects more susceptible to microbial pathogens due to melanin inhibition, immune impairment, and perturbations in microbiota composition, potentially contributing to declines in insect populations.

Key Words: melanin, phenoloxidase, malaria, midgut microbiome, microbiota *Galleria mellonella*, *Anopheles,* vector biology, nodulation, fungi, tyrosinase, hormesis, antioxidant, acid synergism

INTRODUCTION

Melanin, a black-brown pigment found in all biological kingdoms, is produced through a series of oxidation and reduction reactions. These reactions are typically catalyzed by two classes of enzymes: laccases (EC. 1.10.3.2) and phenoloxidases – a family which includes tyrosinases (EC. 1.14.18.1) (1). Tyrosinases are copper metalloenzymes found in bacteria, fungi, protists, arthropods, birds, and mammals (2–7), and have two catalytic roles: 1) hydroxylation of monophenols into *ortho*-diphenols, followed by 2) oxidation of *o*-catechols into *o*-quinones (8). During melanization, tyrosinase converts 3,4-dihydroxyphenylalanine (L-DOPA) to dopaquinone. Dopaquinone undergoes oxidation and reduction reactions to first form dopachrome, then dihydroxyindole. Dihydroxyindole undergoes radical-mediated polymerization to form melanins (8,9).

Melanization is an important component of immunity in virtually all insects (9). Upon infection, protease cascades are activated that cleave pro-phenoloxidases into active phenoloxidases. Phenoloxidases convert catecholamines in the hemolymph into melanin, which surrounds and eliminates the pathogen through exposure to reactive oxygen species (ROS) and lysis from toxic melanin intermediates (3,9–13). This melanization process is a key component of insect immune defense against bacterial, fungal, and protozoan pathogens, nematode parasites, and insect parasitoids (14–21). In addition, pathogens are cleared by two similar processes: nodulation of smaller microbes such as bacteria, fungi, and protozoa, and encapsulation for infections with larger organisms such as helminths and parasitoid eggs (22). Both nodulation and encapsulation involve pathogen neutralization via melanin accumulation and hemocyte (insect “blood cells”) aggregation around the pathogen (22). Melanization and phenoloxidases are also important for wound healing and cuticular development – processes vital for insect health and survival (23,24). Since melanization is an essential physiological process and effector of insect health, understanding how common environmental contaminants affect melanin production is important. The significance of this is also highlighted by findings

suggesting that insect populations may be in decline in recent decades (25).

One ubiquitous chemical found in the environment is glyphosate, the most commonly used herbicide world-wide, which was previously shown to interfere with melanization in the fungus *Cryptococcus neoformans* (26). Glyphosate is a phosphonic glycine analogue and the active ingredient in Roundup herbicides (27). It kills plants through competitive inhibition of EPSP synthase in the shikimate pathway responsible for aromatic amino acid synthesis in many plants, fungi, and bacteria (28). The low cost of glyphosate and wide availability of genetically-modified glyphosate-resistant crops has increased both crop yields and glyphosate-based herbicide use in agriculture (29,30). Between 1996-2014, glyphosate-resistant crops were linked to a 12-fold global increase in glyphosate use, including 8-fold in the US, 134-fold in Brazil, and 107-fold in Argentina (31,32).

In practice, glyphosate is commonly applied at concentrations of ~28 to 57 mM (33) or in formulations of 360 g/L (2 M), with 720 g (4 mol) per hectare (34). Glyphosate-based herbicides are sprayed onto crops where the glyphosate is taken up by plant leaves and translocated to growing tissues throughout the plant (35). Glyphosate is translocated to the roots where it is released into the soil (34). In total, about 88% of the sprayed glyphosate ends up in the topsoil (36–38)(38) . Less than 1% of glyphosate has been shown to enter water bodies, typically following heavy rain, snowmelt, ploughing, or erosion (37), but concentrations from <1 nM to ~30 μM in nearby water have been reported (39). Further, glyphosate has been shown to enter the air through wind erosion and deposit via rain (40).

Glyphosate is remarkably stable, with half-life ranging from weeks to years depending on the surrounding microbial populations, which provide the primary mechanism of glyphosate degradation, while temperature, light, acidity, and salinity also play roles in the degradation process. Microbes mostly break down glyphosate into aminomethylphosphonic acid (AMPA), which persists up to 20 times longer than glyphosate, and is often found in higher concentrations in topsoil and water (41–45).

While glyphosate may have harmful effects on microbes and animals (as reviewed in (35,46)), its impact on environmental microbial communities is inconclusive. Some studies demonstrate clear perturbation of microbial communities, including disrupting rhizosphere composition and fungal endophyte growth and viability (47–50), while others show little to no long term impact on microbial communities (51–53), with no effects on overall soil health or reduction in soil microbial mass (54). Microbial communities are also abundant in insect guts, where they are important for insect health (55–58), and several studies have linked detrimental effects of glyphosate on insect health to disruption of the microbiota. Honeybees exposed to glyphosate have altered microbiomes and are more susceptible to *Serratia marcescens* (59), although AMPA did not have the same effect (60). In tsetse fly midguts, glyphosate disrupts *Wigglesworthia glossinidia's* production of folate - a compound required for tsetse fly health and vector competence for *Trypanosoma brucei* parasites (61).

Beyond effects on microbial communities, glyphosate has broad physiological impacts on insects, other arthropods, and vertebrates. While glyphosate was harmless to *Lepthyphantes tenuis* spiders, it changed behavior and increased mortality in *Pardosa milvina* and *Neoscona theisi* spiders (62–64). Glyphosate reduced learning in *Aedes aegypti* mosquitoes (65) and in honeybees reduced survival and caused learning defects associated with feeding, homing, and flight behaviors (66,67). Glyphosate and AMPA delayed development and reduced survival of the arthropod *Daphnia magna* (68). Glyphosate induces oxidative stress and damage in many organisms, including *D. magna*, insects (fruit flies), amphibians (African clawed frog, European green toad, marsh frog), fish (brown trout, spotted snakehead fish), and mammals (rats) (69–74), often linked with lipid peroxidation and expression of antioxidant defenses (catalase, glutathione, and superoxide dismutase). In human erythrocytes, glyphosate and AMPA mixtures increase ROS production (75,76).

Given the melanin-inhibitory properties of glyphosate in fungi (26), we examined the roles of glyphosate and AMPA as inhibitors of insect melanization and phenoloxidase. We used

two distinct insect models that both rely on melanin-based immunity: *Galleria mellonella* – a species of wax moths (Lepidoptera: Pyralidae), and *Anopheles gambiae* – a mosquito vector of malaria (Diptera: Culicidae). Considering melanin's importance in insect immunity, we evaluated glyphosate's effects on *G. mellonella* susceptibility to the pathogenic fungus *C. neoformans,* and on *A. gambiae* survival and susceptibility to the malaria parasite *Plasmodium falciparum* as measured by parasite oocyst burden. Additionally, we evaluated glyphosate's mechanism of melanin inhibition using L-DOPA auto-oxidation and mushroom tyrosinase-mediated oxidation models. Mushroom tyrosinase is commercially available and produces melanin in a similar mechanism as insect phenoloxidase. The purified enzyme and L-DOPA auto-oxidation allowed us to take a controlled step-by-step biochemical approach to show that glyphosate inhibits melanization by disrupting oxidative balance.

RESULTS

Glyphosate and AMPA Inhibit *Galleria mellonella* Phenoloxidase Activity

In insects, phenoloxidases are activated by serine proteases upon wounding or infection, thus triggering melanin production to either clot a wound or restrict a pathogen (77). To investigate whether glyphosate inhibited insect melanogenesis, we used two models: *G. mellonella* wax moth larvae, and *A. gambiae* adult mosquitoes, a main vector of malaria. In an *ex vivo* analysis using *G. mellonella* hemolymph, we found that glyphosate inhibited phenoloxidase activity in a dose dependent manner, without addition of exogenous substrate (Fig. 1A). Similar results were found with addition of a broad-spectrum protease inhibitor, which was used to control for continued activation of phenoloxidase, glyphosate-induced cellular responses, and/or off-target effects on other components of the phenoloxidase cascade (Supplementary Fig. 1A). We also saw similar inhibition of phenoloxidase activity with the addition of exogenous L-DOPA; however, in these experiments there was only a modest enhancement of phenoloxidase activity with lower glyphosate concentrations followed by

striking inhibition at higher concentrations (Supplementary Fig 1B). Importantly, glyphosate did not impact hemocyte viability, as measured by trypan blue exclusion (Supplementary Fig. 1C). Aminomethylphosphonic acid (AMPA), a primary breakdown product of glyphosate that accumulates in the environment (45), inhibited melanization similarly to glyphosate using *G. mellonella* hemolymph and a commercially available mushroom tyrosinase (Fig. 1B, Supplementary Fig 1D). These data show that glyphosate inhibits melanization in insects similar to what has been previously shown in fungi (26), thus indicating that glyphosate interferes with major melanin-based processes in at least two kingdoms of life.

Glyphosate Alters *G. mellonella* Susceptibility to Infection

Next, we sought to determine whether glyphosate increased *in vivo* susceptibility of *Galleria mellonella* larvae to foreign organisms. We injected *G. mellonella* final instar larvae with 2 µg of glyphosate (~8-12 ng/mg per larvae) followed by infection with *C. neoformans* or a mock infection. The two mock infected groups, glyphosate-treated and phosphate-buffered saline (PBS)-treated exhibited similar survival. However, in the infected groups, the glyphosate-treated larvae died faster compared to the PBS-treated controls (Gehan-Breslow-Wilcoxen test, $p = 0.013$) (Fig. 1C). A similar, but non-significant, trend was seen with a *C. neoformans lac1Δ* strain (Supplementary Fig. 1E). The *lac1Δ* strain is unable to produce melanin, an important virulence factor in *C. neoformans* pathogenesis. This strain is less virulent in the *G. mellonella* model (78), potentially contributing to the lack of significant differences between the glyphosate and PBS-treated groups.

The decreased survival of the glyphosate-treated group infected with *C. neoformans* was correlated with smaller melanized particles within nodules formed during infection (*in vivo*), as compared to the PBS-treated group infected with *C. neoformans* (Fig 1D). For these experiments, we infected and drugged *G. mellonella* as we do during normal infections, then collected the hemolymph 24 hours later and imaged the nodules and aggregates that formed *in*

vivo. The PBS-treated non-infected group had smaller or virtually no melanized structures. In two of three replicates, the PBS-treated infected group had more melanized structures than the glyphosate-treated group (Supplementary Fig 1G-I). Further, in the glyphosate-treated infected group we observed more *C. neoformans* cells, and those within nodules displayed lower degrees of melanin encapsulation compared to PBS-treated larvae (Chi-squared test, p = 0.0034) (Fig 1E). The scoring was based on a system devised with 0 representing no melanin encapsulation of the yeast cell to 4 being the most melanin encapsulation, as depicted in (Fig 1F). The one-time treatment with glyphosate did not disrupt time to larval pupation, a process mediated by laccases and phenoloxidases (Supplementary Fig. 1F). These data suggest a direct correlation between glyphosate treatment, and increased susceptibility of *G. mellonella* to infection caused by decreased melanin-based immune response (nodulation).

Glyphosate Alters *A. gambiae* Phenoloxidases, Susceptibility to Infection with Malaria Parasites, and Survival

To ascertain the impact of glyphosate on *Anopheles gambiae* mosquito melanization, we measured the phenoloxidase activity in whole-body mosquito homogenate following the addition of glyphosate. Similar to our results with *G. mellonella*, glyphosate inhibited phenoloxidase activity of *A. gambiae* homogenate in a dose-dependent manner (Fig. 2A).

To investigate whether glyphosate rendered mosquitoes more susceptible to infection with the human malaria parasite *P. falciparum*, adult female mosquitoes were fed on 10% sugar solution supplemented with glyphosate at different concentrations for 5 days and then given a *P. falciparum*-infected blood meal. Parasite burden was assessed through enumeration of the *Plasmodium* oocyst stage at 8 days post infection (DPI). Glyphosate-fed mosquitoes had higher oocyst burdens with an overall non-significant trend of increasing oocyst burden with increasing dose of glyphosate (Fig. 2B). However, we observed a sharp decline in parasite burden in the 10 mM treated group, which was likely due to the increased mortality of this group (Fig. 2C)

resulting in few surviving mosquitoes to assess the intensity of infection. In a low *P. falciparum* infection intensity assay (Supplementary Fig. 2A), we observed that glyphosate-treated groups are more likely to be infected than control groups. This is important, as lower parasite burdens are more reminiscent of infections in field conditions in malaria endemic regions (79–82).

Sugar preparations with glyphosate at environmentally relevant concentrations were given to *A. gambiae* mosquitoes to ascertain the herbicide's effect on the mosquito's lifespan. Compared to control mosquitoes (sugar-fed without glyphosate), mosquitoes given low glyphosate doses (30 to 300 μM) showed statistically significant improved survival, while those fed higher doses of glyphosate (1 to 10 mM) had equal or decreased survival, with the 10 mM glyphosate-exposed group exhibiting significantly decreased survival (Fig. 2C). Additionally, we used a Cox Mixed Effects Model to account for fixed and random effects, and calculated the Hazard Ratios for each of the treatment groups (Fig. 2D). Hazard Ratios<1 indicate a reduced risk of death compared to the control while Hazard Ratios>1 indicate enhanced risk of death compared to the control group. With this model, the mosquitoes treated with lower glyphosate concentrations had a Hazard Ratio less than 1, those treated with 1 and 3 mM glyphosate had Hazard Ratios similar to 1, and the 10 mM-treated mosquitoes had a Hazard Ratio significantly greater than 1. These results suggest that glyphosate could have bimodal effects on mosquito health.

We also measured the impact of glyphosate on the mosquito cuticle and body size. There was no discernable difference in *A. gambiae* cuticle pigmentation after 5 days of treatment with 1 mM glyphosate in 10% sucrose from days 3 to 8 post-emergence, as measured by mean gray value of the ventral abdomen (Supplementary Fig. 2C). This was expected due to the typical expression of cuticular laccases being largely at the timing of pupation and the first three days post-emergence (23,24). Additionally, there were no difference in wing length, a proxy for adult size, between the glyphosate-treated and untreated adult mosquitoes (Supplementary Fig. 2D). Altogether, this suggests that the observed increased

parasite burden in glyphosate-treated mosquitoes cannot be explained merely by broader impacts of glyphosate on mosquito health.

Glyphosate Alters the Composition, but Not Density, of the *A. gambiae* Midgut Microbiota

A. gambiae midgut microbiota can influence *Plasmodium* infection by modulating the mosquito's innate immune system and hence affecting parasite viability (83–86). We investigated whether glyphosate had detrimental effects or influence on the *A. gambiae* microbiota. Colony Forming Unit (CFU) counts from cultures of midgut homogenates grown on LB agar demonstrated that glyphosate treatment did not affect total number of culturable gut bacteria (Fig. 3A), though this method would miss any impacts on microbes that were not readily cultured by these methods. To complement our culture-dependent analysis and provide insight on microbiota community composition, we compared the total 16S rRNA composition of the midgut microbiota with and without glyphosate treatment. Glyphosate treatment altered microbiota composition, with a noted decrease in the relative abundance of Enterobacteriaceae and an increase in relative *Asaia spp.* populations (Fig. 3B). We did not observe a dose-dependent impact on composition, as the alpha diversity (a function of the number of bacterial taxa) of mosquitos exposed to glyphosate was similar to controls (Fig. 3C). However, community composition was perturbed by treatment with glyphosate, and glyphosate-treated groups and controls form two separate clusters in principal coordinates analysis as measured by Bray-Curtis dissimilarity (Fig. 3D). These differences suggest a shift in beta diversity (prevalence of each bacterial taxon), and therefore a difference between the microbial communities of mosquitoes exposed to glyphosate versus untreated controls.

Glyphosate Inhibits Production of Dopaquinone, Dopachrome, and Melanin

To understand how glyphosate inhibited melanization, we evaluated the formation of melanin intermediates in a stepwise manner using a commercially available fungal tyrosinase

and the melanin precursor L-DOPA (2 mM). Although this tyrosinase differs from insect phenoloxidase, the melanization reaction in these systems follows the same Mason-Raper pathway (Figure 4A) (87,88) and thus can be used to explore the mechanism of glyphosate inhibition. The first step of the reaction involves L-DOPA oxidation to dopaquinone (DQ) enzymatically or spontaneously (89). We found that glyphosate inhibited the dopaquinone production in a dose-dependent manner (Fig. 4B). This inhibition was observed for both tyrosinase-mediated and auto-oxidation-mediated production of dopaquinone. The slopes of inhibition in the auto-oxidation and tyrosinase-mediated oxidation were similar. This indicated that the tyrosinase reaction dopaquinone levels would remain unchanged by glyphosate treatment if the inhibition of "background" auto-oxidation dopaquinone production were taken into consideration. These results suggested that dopaquinone inhibition was primarily rooted in preventing the oxidation of L-DOPA independent of tyrosinase.

Dopaquinone spontaneously cyclizes to form cyclodopa, which then undergoes a redox exchange with another dopaquinone molecule to form one molecule of dopachrome and one reformed molecule of L-DOPA. Dopachrome is a pink-orange melanin intermediate that has an absorbance maximum at 475 nm. Dopachrome is a useful proxy product for tyrosinase-mediated reaction kinetics and evaluating the melanization reactions and redox exchange (90). The rate of dopachrome formation and the amount of dopachrome produced were determined by measuring changes in absorbance during a reaction between L-DOPA and tyrosinase. There was a strong dose-dependent inhibition of dopachrome formation with glyphosate (Fig. 4C), implying that the compound's inhibitory effects were upstream of dopachrome.

We tracked the reaction over 5 d to confirm inhibition of melanin synthesis. Glyphosate inhibited the production of a black pigment dose-dependently, as measured by the absorbance of the tyrosinase reaction on Day 5 (Fig. 4D). Interestingly, glyphosate also inhibited the formation of pigment that derives from auto-oxidation of L-DOPA (Fig. 4D). This implies that glyphosate inhibited pigment production non-enzymatically.

Phosphate-Containing Compounds Inhibited Melanization Similarly to Glyphosate

To gain insight into the chemical features of glyphosate that inhibited melanogenesis we assayed several structurally similar compounds using the same *in vitro* mushroom tyrosinase assay. To test the effect of the amino acid functional group, we compared glyphosate alongside its non-phosphate analog, glycine. We also tested the inhibitory effects of phosphoserine and serine on melanin production. Phosphoserine inhibited dopaquinone, dopachrome, and melanin formation to nearly the same extent as glyphosate (Fig. 5A-C). In contrast, neither glycine nor serine inhibited dopaquinone, dopachrome, or overall melanin formation (Fig. 5A-C). We tested the inhibitory effects of other phosphate-containing compounds including organophosphates (phosphonoacetic acid), phosphoesters (pyrophosphate), and phosphoric acid. All of the phosphate-containing compounds inhibited dopaquinone production (Fig. 5A) and dopachrome formation (Fig. 5B) in a manner nearly identical to glyphosate, but differed slightly from each other in melanin inhibition (Fig 5C).

Similar to glyphosate, these compounds all inhibited auto-oxidation of L-DOPA comparably to their inhibition of tyrosinase-mediated melanin production (Fig. 5E). This further illustrates that glyphosate and similar phosphate-containing compounds inhibit melanin in a non-enzymatic fashion. These data suggest that the phosphate functional groups of these compounds may be responsible for the melanin-inhibitory properties.

Glyphosate Does Not React With L-DOPA or Inhibit Tyrosinase Directly

We considered the possibility that glyphosate inhibited melanogenesis and dopaquinone production by reacting with the L-DOPA substrate. To measure the reaction between these compounds, we analyzed mixtures of L-DOPA and glyphosate by ^{1}H-NMR and ^{31}P-NMR. We found no evidence of interaction between the two compounds based on peak shifts of hydrogen

297 and phosphorous at both high (60 mM glyphosate and 20 mM L-DOPA) and low concentrations
298 (6 mM glyphosate and 5 mM L-DOPA) (Supplementary Fig. 4).
299 If glyphosate was inhibiting melanin production through the formation of a covalent bond
300 with tyrosinase, the inhibition should be irreversible. To test this, we treated 20 µg/ml tyrosinase
301 with 5.63 mg/ml (33.33 mM) glyphosate and removed the glyphosate by dialysis. The
302 glyphosate-treated enzyme had similar activity to the control (Fig. 6A), making a strong case
303 against a mechanism whereby glyphosate inhibited melanogenesis through irreversible
304 inhibition of tyrosinase. Instead, analysis of the tyrosinase reaction by Michaelis-Menten kinetics
305 assay with L-DOPA and glyphosate suggested that glyphosate is a non-competitive inhibitor of
306 melanin and dopachrome production (Fig. 6B). Further, we tested tyrosinase activity as a
307 function of enzyme concentration with and without glyphosate and constant concentration of L-
308 DOPA. We found that the slope of the glyphosate-treated enzyme is lower than the water-
309 treated control (Fig. 6C). This indicates that glyphosate-mediated inhibition is reversible (91,92).
310 Given that our findings showed that glyphosate inhibits auto-oxidation and tyrosinase-mediated
311 oxidation, we believe that the reversible inhibition is due to glyphosate interfering with the L-
312 DOPA substrate's ability *to be* oxidized rather than the enzyme's ability *to* oxidize. This could be
313 represented by the following where *E* represents tyrosinase, *S* represents L-DOPA, *I* represents
314 glyphosate, and *P* represents dopaquinone/melanin:

315 Normal Enzymatic Reaction: $E + S \rightleftharpoons ES \longrightarrow P$

316 Inhibited Enzymatic Reaction: $E + S + I \rightleftharpoons E + SI \dashv P$

317 Copper ions are important for tyrosinase activity. Since glyphosate is a metal chelator
318 (93,94) , we evaluated whether glyphosate's inhibitory effect was due to this property. We added
319 copper ions to the L-DOPA and tyrosinase reaction to rescue the glyphosate inhibition. We
320 performed the experiment with eight concentrations of copper (II) sulfate for each of the eight
321 glyphosate concentrations. In general, the addition of copper did not rescue the glyphosate
322 dependent inhibition of melanin (Fig. 6D). However, low concentrations of copper (6.25 - 25 µM)

increased tyrosinase activity, while high concentrations of copper (50 - 400 μM) reduced activity, indicating low copper can boost enzyme activity, while higher concentrations inhibit the reaction. However, this hormesis-like effect was not observed at increasing glyphosate concentrations (Supplementary Fig. 5). This result indicates that glyphosate's ability to chelate copper ions could have a protective effect in high copper environments, which would otherwise lead to negative effects on enzymatic activity and other biological processes. Similar results have been previously seen in *Eisenia fetida* earthworms exposed to high copper conditions in soil (95). Glyphosate contamination of copper-rich soil reduced the detrimental effects of the metal's toxicity, presumably due to the glyphosate's copper chelation properties (95).

Glyphosate Affects the Oxidative Properties of Melanogenesis

Melanogenesis is dependent on the spontaneous radicalization of quinone intermediates (96). Dopaquinone radicals and cyclodopa undergo a radical-mediated redox exchange that converts cyclodopa into dopachrome and dopaquinone into L-DOPA. Further downstream, ROS catalyze the polymerization of dihydroxyindole into eumelanin. Glyphosate's inhibitory effect could be due to a role as a free-radical scavenger or antioxidant. Since the inhibitory compounds blocked spontaneous oxidation of L-DOPA (Fig. 5E), they are antioxidants. To measure this radical-quenching ability we used an ABTS assay in which ABTS radicals are blue, but when quenched the solution becomes colorless. The degree of discoloration is a proxy for radical concentration and antioxidant strength. Glyphosate quenched the ABTS radical to some degree, but only after several hours of reaction (Supplementary Fig. 6A), which did not occur with the other inhibitory phosphate-group containing compounds evaluated (Fig. 7A). This indicates that direct free-radical scavenging may not be the primary mechanism of melanin inhibition for glyphosate.

Phosphoric acid is a well-known synergist that boosts the antioxidant properties of phenolic compounds. Phosphoric acid, and other synergists such as citric acid, malic acid, and

tartaric acid do not directly quench free radicals themselves, but instead work by regenerating antioxidants, thus becoming “sacrificially oxidized”, or chelating metal ions in solution (97,98). Alternatively, glyphosate could be reacting with existing antioxidants to strengthen and/or regenerate them into “active” form. In this instance, the glyphosate would be bolstering the antioxidant properties of L-DOPA.

We observed that the synergist citric acid inhibited melanization similarly to glyphosate and phosphoric acid (Fig. 7B,C). The addition of glyphosate, phosphoserine, and phosphoric acid enhanced the antioxidant properties of L-DOPA in an ABTS assay in a similar manner as citric acid (Fig. 7D). This suggests that glyphosate may act as an inhibitor via antioxidant synergism. The synergy is the ratio of the quenching capacity of the L-DOPA and the compounds alone to the quenching capacity of L-DOPA combined with the compound. The lower this ratio, the more synergistic the compounds are with L-DOPA (Supplementary Fig. 6B). These values indicate that the inhibitory compounds are synergistic, whereas the non-inhibitory glycine and serine are not as synergistic.

The inhibition of melanin was independent of the L-DOPA to glyphosate ratio, and glyphosate’s IC_{50} is ~1 mM regardless of L-DOPA concentration (Supplementary Fig. 7). This could be explained by a general antioxidant effect on solution.

Glyphosate Alters the Oxidation-Reduction Potential of the System

L-DOPA is a more effective antioxidant when it is oxidized or radicalized, and has a better ability to form adducts with other radicals (99). Since glyphosate is acting as a synergistic antioxidant, it may be driving L-DOPA oxidation and possibly radicalization in which L-DOPA scavenges radicals better. This has the potential to disrupt melanin synthesis by stopping the spontaneity of redox exchange and dopaquinone formation.

To investigate whether the addition of glyphosate changed the oxidation properties of L-DOPA, we used cyclic voltammetry – a technique to measure the electrochemical properties of

375 solutions and previously used to study quinone electrochemistry (100,101). Voltammetry
376 performed on L-DOPA solutions with glyphosate showed dose-dependent shifts towards a
377 negative potential (Fig. 7E,H) in peaks that corresponded to L-DOPA oxidation (102) (**Peak 1**).
378 We validated these as L-DOPA oxidation peaks by performing voltammetry on various L-DOPA
379 concentrations **(**Supplementary Fig. 8A). The peak shift towards negative potentials indicates
380 the L-DOPA was oxidized more easily and had less ability to be an oxidant, similar to the
381 negative potential shifts associated with alkaline pH and increased oxidation (103). We
382 controlled for any pH-dependent peak shifts by adjusting each solution to pH 6.00 prior to
383 measurement. Decreased oxidizing power can lead to significant effects, as melanin
384 biosynthesis is reliant upon catechol oxidation and high redox potentials of quinones.
385 Interestingly, with increased glyphosate, the L-DOPA solution had a lower current intensity
386 associated with the reduction of dopaquinone to L-DOPA (**Peak 2)**. In cyclic voltammetry,
387 smaller peaks indicate that less of the compound is oxidized or reduced. The decreased **Peak 2**
388 current became virtually non-existent with increasing glyphosate concentrations (Fig. 7E,H,I).
389 This implies that dopaquinone, represented by **Peak 2**, is either not being formed during L-
390 DOPA oxidation or cannot be reduced back into L-DOPA. These data indicate that the redox
391 cycling steps of melanization are halted due to the inability of dopaquinone to be reduced into L-
392 DOPA. This could also indicate that while L-DOPA was oxidized more in the presence of
393 glyphosate, it may form a non-dopaquinone product - either a radical-mediated dimer with itself
394 or a semiquinone.

395
396 **DISCUSSION**

397 We investigated the effect of glyphosate on melanin production in two species of insects,
398 *Galleria mellonella* and *Anopheles gambiae*, and found that both glyphosate and its major
399 metabolite AMPA were inhibitors of insect phenoloxidase and melanization. Although
400 glyphosate and AMPA are relatively weak inhibitors of these insects' melanization, the inhibitory

401 concentrations are relevant in the environment given the vast amounts used in agriculture, their
402 environmental stabilities, and the high potential for insect-herbicide interactions. Therefore,
403 glyphosate has a high potential to influence key insect physiological systems. We observed that
404 glyphosate enhanced the susceptibility to infection of two phylogenetically distinct insects, *G.*
405 *mellonella* and *A. gambiae*. This raises concerns and the suggestion that glyphosate may
406 interfere broadly with insect immunity through its effects on melanin-based defenses. Analysis
407 of *in vitro* tyrosinase and auto-oxidation models revealed that glyphosate inhibited melanization
408 by acting as a synergistic antioxidant and disrupting redox cycling. Overall, our findings provide
409 new insights on the complex reaction and suggest potential harmful effects of this herbicide on
410 non-target organisms, including some insects that may be important to ecosystem stability, and
411 already in peril due to the threat of an “insect apocalypse”.

412 *G. mellonella* treated with glyphosate were more susceptible to infection with *C.*
413 *neoformans*. Glyphosate treatment was associated with reduced size of melanized nodules in
414 the hemolymph following infection with *C. neoformans*. Two of three replicates showed
415 significantly reduced numbers of melanized nodules in the glyphosate-treated infections.
416 Nodules are primarily composed of hemocyte aggregates, released immune factors, and
417 melanin encapsulation of the pathogen, which function together to kill invading pathogens (22).
418 Altogether, these data suggest that glyphosate weakened the melanin-based immune response
419 of *G. mellonella,* which could have grave implications for host defense. *Galleria* are members of
420 the order Lepidoptera (moths and butterflies), which represent up 10% of known species on
421 Earth. Interactions with glyphosate in the soil, on plants during pollination, or ingested through
422 herbivory could contribute to immunocompromised lepidopteran populations. Glyphosate’s
423 effects on immunity in insects could compound a controversial and pre-existing problem of
424 declines in Lepidopteran biomass in recent decades (25,104–107).

425 Like our observations with *G. mellonella*, glyphosate made the *A. gambiae* mosquito
426 more susceptible to *P. falciparum* parasite infection, the primary agent of human malaria in

Africa. However, melanization is not considered the primary anti-*P. falciparum* immune response in this malaria model (108). The increased susceptibility of *A. gambiae* to *P. falciparum* could be due to broader alterations of mosquito immune defenses, or disruption of non-melanin roles of catecholamine oxidation and phenoloxidase in insect immunity including the production of ROS, cytotoxic intermediates, and pathogen lysis (3,13,109). Importantly, we observed that even when infections of *A. gambiae* with *P. falciparum* resulted in an overall low to no parasite burden in control-treated groups, glyphosate-treated groups exhibited a higher infection burden and prevalence. This is notable because *Plasmodium* oocyte development within the mosquito is a major bottleneck to successful vector competence in nature (110). If a mosquito can prevent oocyst formation, there is no transmission of malaria to humans. The numbers of oocysts from these low parasite burden experiments are in line with the normal burden's found in natural field infection models (111,112). Our data may indicate that mosquitoes exposed to glyphosate were less able to control *Plasmodium* infection they would have otherwise resisted, thereby becoming potentially better vectors for malaria. Overall our results raise concerns for public health and malaria control initiatives in regions in which malaria is endemic and where there is increasing use of glyphosate, including areas of Latin America, Sub-Saharan Africa, and Asia.

Our data revealed that uninfected adult female mosquitoes treated with glyphosate displayed a hormesis-like dose-dependent effect when measuring survival outcomes. Survival increased at low doses of glyphosate compared to the control. This greater longevity may be due in part to reduced basal damage from host defense mechanisms that normally occur during melanin formation, and/or altered gut microbiota. In contrast, mosquitoes exposed to high concentrations of glyphosate showed decreased survival. These data suggest the broader notion that glyphosate could have varied and complex outcomes on vector competence depending on its concentration in the environment. The low-concentration glyphosate treatments resulted in longer-lived, yet immunosuppressed, mosquitoes that were slightly more

susceptible to infection with *P. falciparum,* whereas short-lived high glyphosate treated mosquitoes were much more susceptible to *P. falciparum.* Further, while the 10 mM-treated mosquitoes had the worst survival outcome, the mosquitoes that survived the drugging showed low susceptibility to *P. falciparum* infection. These observations suggest a potentially interesting effect whereby very high concentrations of glyphosate reduce mosquito survival, but bolster the immune system or general physiology of survivors, which then allows them to resist *P. falciparum* infection with greater success. Alternatively, very high glyphosate treatment could be selecting for mosquitoes within the population more resistant to *P. falciparum* infection.

Our analyses of *A. gambiae* midgut microbiota indicated that glyphosate did not impact *A. gambiae* midgut culturable bacterial density; although the herbicide did perturb midgut microbiota composition in a non-dose dependent manner. More specifically, glyphosate altered diversity of the microbial community, and glyphosate-treated mosquitoes exhibited diminished Enterobacteriaceae and expanded *Asaia spp*. populations. The presence of some Enterobacteriacae, including the common insectary contaminant *Serratia marcescens,* in *Anopheles* spp. midguts is associated with lower susceptibility to *Plasmodium spp.* infection (113,114). This effect is observed quantitatively by the significantly different prevalence of individual bacterial taxons (beta diversity) between the glyphosate and control-treated microbiota, while there is an overall unchanged number of bacterial taxa present (alpha diversity). Beta diversity analysis indicates that microbial communities associated with glyphosate-treated mosquitoes cluster together and are different than those from control mosquito communities.

Our results are consistent with reports that glyphosate perturbs the microbiota of honeybees that makes them more susceptible to infection (59). Our data suggests that while glyphosate may perturb the microbiota and affect immunity as previously described (59,60), it can also inhibit melanization which is a critical part of insect immune defense. We do not see a

dose-dependent effect of glyphosate on the microbiota composition, but we do see a dose-dependent effect on mosquito susceptibility to *Plasmodium* infection; this indicates that the enhanced susceptibility might be unrelated to microbiome perturbations. These mechanisms of susceptibility are not mutually exclusive and could be additive to weaken insect health. Additionally, while AMPA does not to disrupt the microbiota of honeybees (60), we show it can inhibit melanization of *G. mellonella* phenoloxidase and mushroom tyrosinase. A recent study in *Apis cerana cerana* honeybees indicate that glyphosate-based herbicide treatment increases expression of wound and defense genes, including those related to melanization (115). Interestingly, this study also showed that glyphosate feeding decreased the expression of many odorant binding proteins, which have been shown to mediate the melanization response in both Tsetse fly (*Glossina morsitans morsitans*) and *Drosophila melanogaster* (116) This suggests complex regulation of melanization following treatment with glyphosate-based herbicide, including the possibility of increased melanin-related gene expression as a compensation for glyphosate's inhibitory effects. Additionally, other surfactants and components of the commercial herbicide formulation used could trigger damage and immune gene expression.

Melanins and phenoloxidases are involved in other physiological functions in insects including proper pupation, and cuticle and eggshell development. In our experiments, which involved single dosing or short duration of feeding, we did not detect a difference in coloration of adult mosquito treated with glyphosate, nor a defect in *G. mellonella* pupation following glyphosate treatments of final instar larvae. However, we cannot rule out that longer glyphosate exposure or feeding throughout the lifecycle would effect these functions. If such effects happen, they will only compound the effects of glyphosate on melanin-based immunity and insect physiology.

We sought to understand the mechanism of melanization inhibition by glyphosate. The process of melanization is highly dependent upon oxidation and redox cycling between catechols and quinones. The melanin production process is halted if the oxidizing ability and the

redox potentials are altered. Melanization begins with the conversion of L-DOPA into dopaquinone through enzymatic or spontaneous oxidation of L-DOPA, followed by redox cycling that results in dopachrome formation, and subsequently melanin polymerization. Glyphosate inhibited formation of dopaquinone and melanin pigment mediated by both tyrosinase and auto-oxidation, which strongly suggests that glyphosate inhibits L-DOPA oxidation in an enzyme independent manner. We found that other phosphate-containing compounds inhibited melanization in a similar manner including phosphoserine, phosphoacetic acid, pyrophosphate and phosphoric acid. This is in line with literature reports that other aminophosphonic acids inhibit fungal eumelanin in the human pathogen *Aspergilius flavus* (117). Incidentally, this class of compounds is patented for use in human cosmetics, and are marketed as solutions to inhibit melanogenesis in the skin (118,119).

We found no evidence that glyphosate irreversibly inhibited tyrosinase activity or directly interfered with enzyme function. Addition of copper ions did not rescue the inhibition, indicating that the copper-based catalytic core of tyrosinase in not disrupted by glyphosate. Interestingly, low copper increased tyrosinase activity and high doses reduced activity. However, copper had minimal effects on tyrosinase activity during high glyphosate concentrations. It appears that glyphosate, possibly through chelation, acts as a “buffer” of copper ions and can reduce the metal’s harmful effects, similar to previous findings concerning the toxicity of high-copper soil to earthworms following glyphosate treatment (95). This could have broader implications for melanogenesis in nature, where some fungi use copper as a signal to upregulate melanin-producing enzymes (120), and thus copper ion sequestration could reduce melanin production.

We examined the ability of glyphosate and the other compounds to quench free radicals, which are necessary to the melanization process. Of the inhibitors tested, only glyphosate had radical-quenching activity, but this occurred relatively slowly compared to the typical timeframe of antioxidant reactions reported in literature (121). This property is likely not the mechanism of inhibition as phosphoserine has a similar structure and near identical inhibition of melanization

as glyphosate, yet no radical-quenching properties. While not a free-radical quencher, phosphoric acid is a known antioxidant synergist – a class of compounds that enhance antioxidant properties of phenolic compounds by chelating metals or reverting antioxidants into their active states (98). Synergists like phosphoric acid, citric acid, malic acid, and alpha-hydroxy acids are added to foods, medicines, and cosmetics at concentrations up to 10% as a preservative due to their synergist effects on antioxidants (122). Glyphosate behaved similarly to phosphoric acid and citric acid; citric acid inhibited melanization similarly to glyphosate and phosphoric acid, suggesting an inhibition mechanism via antioxidant synergy. Additionally, we report that glyphosate and other inhibitors have synergistic effects on the antioxidant properties of L-DOPA. L-DOPA's antioxidant properties derive from its reduction back to a normal state from an oxidized state, or a radical-mediated adduction reaction with the oxidized compounds in solution. Since glyphosate makes L-DOPA a more efficient antioxidant, glyphosate thus alters the oxidative balance of L-DOPA and/or produces a buildup of radical or semiquinone intermediates.

Consistent with these findings of antioxidant synergy, cyclic voltammetry revealed that glyphosate decreased the L-DOPA-Dopaquinone redox potential. Hence, L-DOPA becomes both a weaker oxidizing agent and a stronger reducing agent (antioxidant) and is more prone to oxidation in the presence of the herbicide. Glyphosate decreased dopaquinone reduction in a dose dependent fashion indicating that dopaquinone cannot be reduced or is not produced following L-DOPA oxidation. A lack of dopaquinone could indicate that glyphosate causes oxidized L-DOPA semiquinone intermediates to remain stable or react with each other and form L-DOPA dimers. On the other hand, if dopaquinone cannot be reduced into L-DOPA, melaninization becomes unfavorable as redox exchange could not occur. These changes in voltammogram do not appear when the L-DOPA solution is treated with 16 mM glycine, but did occur with citric acid. This further supports that glyphosate is acting as a synergistic antioxidant and prevents the redox-dependent melaninization.

Our findings investigating glyphosate's mechanism of melanin inhibition points to disruption of oxidative balance and redox cycling which may result in the buildup of toxic oxidative intermediates. Previous studies evaluating glyphosate's impact on organisms show that the herbicide increases oxidative stress, lipid peroxidation, and antioxidant responses in bacteria, plants, arthropods, fish, amphibians, rats, and human red blood cells (69–76). These data bolster our findings that glyphosate promotes oxidation in phenolic compounds like L-DOPA and inhibits clearance of oxidative stress. Understanding the mechanisms by which compounds such as glyphosate might impact insect biomass and contribute to a potential insect decline is important, as they have both direct and indirect impacts on human health.

Glyphosate's interference with melanization could have considerable environmental impact given its stability and wide concentration range, from over 50 mM at time and at site of application to under 1 nM in runoffs from application sites (33,39,123). At higher concentrations, glyphosate could inhibit melanin production in some insects, thus rendering them more susceptible to pathogens due to reduced immune competence. This suggests protean consequences for human health ranging from ecosystem disruption to altered vector competency of lethal human pathogens and increased malaria transmission in endemic regions that use glyphosate-based herbicides in agriculture. Importantly, we provide evidence that glyphosate enhances *A. gambiae* susceptibility to the human malaria parasite, which could potentially make it a better vector for transmitting disease to humans. Our data in *Galleria* and *Anopheles* can perhaps be extrapolated to other lepidopteran (moth and butterfly) and dipteran (fly) species with additional importance to the environment.

In summary, our results suggest that glyphosate interferes with melanization in two insect species, through a mechanism involving altering the redox potential of melanin polymerization reaction. This phenomenon is concerning because of the importance of melanization in insect immunity. A strong immune response is vital for insect survival, and disruption of their immune function, including the inhibition of melanization, could be disastrous

582 for these animals. Insects are pivotal members of the world's ecosystems, essential to
583 maintaining proper function, and they ensure human food security. Yet, certain data indicates a
584 drop in insect biomass over recent decades, a phenomenon that has been called the "insect
585 apocalypse" (25,104,105,124,125). Although this view has been questioned regarding the true
586 extent and possible causes of the insect population declines (126–130), our results suggest that
587 glyphosate use as a mechanism by which insect immunity can be undermined by human
588 activities.
589
590 **ACKNOWLEDGEMENTS**
591 We would like to acknowledge Dr. Gene Fridman in the Johns Hopkins School of
592 Medicine for lending the use of the Fridman lab's Metrohm Autolab potentiostat for use in the
593 cyclic voltammetry experiments. We would like to thank the Johns Hopkins Malaria Research
594 Institute and the Department of Molecular Microbiology and Immunology Insectary and Parasite
595 Core facility, and Dr. Joel Tang from the Johns Hopkins NMR Core facility for his help with the
596 NMR experiments. We would also like to thank the entire Casadevall Lab for their suggestions
597 and inputs during conversations and their feedback during lab meetings and presentations.
598 Figures in Supplementary Figure 9 were made using BioRender. DFQS, EC, and AC are funded
599 by the Johns Hopkins Malaria Research Institute Pilot Grant Casadevall_123; DFQS, EC, and
600 AC are funded by NIAID R01 AI052733; DFQS has been funded by NIH grants
601 5T32GM008752-18 and 1T32AI138953-01A1; AJB and NAB are funded by NIH grant National
602 Institutes of Health R35GM128871.
603
604 **AUTHOR CONTRIBUTIONS**
605 D.F.Q.S. contributed to conceptualization, methodology, formal analysis, investigation, data
606 curation, writing of the original draft and subsequent editing, data visualization, and project
607 administration. E.C. contributed to conceptualization, methodology, investigation, resources,

608 reviewing and editing of manuscript, supervision, project administration, and funding acquisition.
609 R.T. contributed to conceptualization, methodology, resources, reviewing and editing of
610 manuscript, and supervision. A.J.B. contributed to conceptualization, methodology, software
611 use, formal analysis, investigation, data curation, reviewing and editing of manuscript,
612 visualization, and project administration. Y.D. contributed to methodology and reviewing and
613 editing of manuscript. G.D contributed to reviewing and editing of manuscript, resources, and
614 funding acquisition. N.A.B. contributed to conceptualization, methodology, investigation,
615 resources, reviewing and editing of manuscript, supervision, project administration, and funding
616 acquisition. A.C. contributed to conceptualization, methodology, resources, supervision, project
617 administration, and funding acquisition.
618
619 **DECLARATION OF COMPETING INTERESTS**
620 The authors declare no competing interests.
621
622 **METHODS**
623 **Biological materials**
624 *Galleria mellonella* larvae were obtained through Vanderhorst Wholesale Inc, St. Marys,
625 Ohio, USA. *Cryptococcus neoformans* strain H99 (serotype A) was kept frozen in 20% glycerol
626 stocks and subcultured into Sabouraud dextrose broth for 48 h at 30°C prior to each
627 experiment. The yeast cells were washed twice with PBS, counted using a hemocytometer
628 (Corning, Inc), and adjusted to 10^6 cells/ml.
629 *Anopheles gambiae* (Keele strain) mosquitoes were maintained on sugar solution at
630 27°C and 70% humidity with a 12 h light to dark cycle according to standard rearing condition.
631 *Plasmodium falciparum* NF54 (Walter Reed National Military Medical Center, Bethesda)
632 infectious gametocyte cultures were provided by the Johns Hopkins Malaria Research Institute
633 Parasite Core Facility and were diluted to 0.05% gametocytemia with naïve human blood before

feeding to the mosquitoes using an artificial glass membrane feeder as established in (Dong et al., 2009) (83).

Compound and Dilution Preparation

Each compound, including the glyphosate (Millipore Sigma, Product #45521), was prepared in 300 mM stock solution in Milli-water Q and brought to a pH of 5.5, and 20 µl of each compound was serially diluted 1:2 in PBS (pH 7.4), with a compound-free control. When all reaction components are added, the final concentrations of the compounds in these dilutions were 33.33, 16.67, 8.33, 4.17, 2.08, 1.04, 0.52, and 0 mM.

***Galleria mellonella* Hemolymph Extraction and Phenol Oxidase activity**

Healthy (active and cream-colored) larvae were cold anesthetized, punctured in their proleg with 18G needle and pressure was applied to the larvae to promote bleeding of hemolymph. Hemolymph was collected from larvae directly into an eppendorf tube. Anticoagulants were not used as they might interfere with the melanization process.

For automelanization experiments, hemolymph was diluted 1:10 in PBS and mixed with a pipette. Then, 160 µl of 1:10 hemolymph is added to 20 µl of glyphosate serially diluted in PBS. The change in absorbance at 490 nm was recorded and analyzed as described above.

For experiments with L-DOPA, hemolymph was diluted 1:5 in PBS and mixed by pipette. Experiments were performed as per the phenoloxidase activity assay in (Cornet, Gandon, and Rivera, 2013 (131)) .

To test the effect of glyphosate on hemocytes viability, hemolymph was diluted 1:2 with anticoagulation buffer (132), as melanization was not of importance for this experiment. Hemocytes were pelleted and suspended in anticoagulation buffer. Glyphosate was added to an aliquot of hemocytes in solution and incubated with mixing on a rocker at 30°C for 15 min. Hemocyte viability was assessed by 0.02% trypan blue staining and enumeration of stained (dead) versus unstained (alive) hemocytes with a hemocytometer.

***Galleria mellonella* Infection and Survival**

Healthy final instar *G. mellonella* larvae weighing between 175 and 225 mg were selected, and left starving overnight. Groups of larvae were injected with 10 µl of PBS or 10 µl of 1 mM sterile glyphosate in PBS. Larvae were monitored and left to recover for 5 h. Larvae were then injected with 10 µl of sterile PBS or injected with 10^4 *Cryptococcus neoformans* yeast cells per larva. Due to the low concentration of glyphosate administered to the larvae, their volume of hemolymph, and their body volume, we believe the approximate concentration of glyphosate is below the concentrations required to inhibit *C. neoformans* growth (26). *G. mellonella* larvae and pupae were kept at 30°C and monitored daily for survival for 14 d. Survival was assessed by movement upon stimulus with a pipette. See Supplementary Fig. 9a.

Melanization and Nodule Measurements

G. mellonella larvae were drugged and infected as described above in groups of 3 larvae per condition. After 24 h, larval hemolymph was removed directly in anticoagulation buffer, centrifuged at 10,000 *xg* for 5 min, and resuspended in coagulation buffer.

Brightfield microscopy images were randomly taken at 4x magnification, with 15-20 images taken per condition per replicate. These images were analyzed using Fiji (133) Particle Analyzer function using with a threshold set between 0 and 120 mean gray value. Particle area and numbers were calculated. Additional images were taken of nodules at 20x and 100x magnification, the latter of which were used to manually score the degree of melanization of fungal cells within the nodules. Statistical significance of differences between melanized particle area was analyzed using a nested non-parametric Mann-Whitney-Wilcoxon rank test using the *nestedRanksTest* package (*Version 0.2*, D.G. Scofield , 2014)(134) in R for R 4.0.2 GUI 1.72 for Mac OS at https://www.r-project.org/ (R Core Team, 2020).

***Anopheles gambiae* Phenol oxidase activity**

Phenoloxidase activity assays were performed as previously described (135). Experiments were done in biological triplicate with different batches of mosquitoes, as well as in technical triplicate per biological replicate of 3 batches of 10 mosquitoes.

686 ***Anopheles gambiae* Survival**

687 Adult female mosquitoes of *A. gambiae* Keele strain were raised on 10% sucrose for
688 three days post-emergence. On the third day, adult females were sorted into seven groups of 40
689 and placed into mesh-covered cardboard cups and provided a cotton ball with 10% sucrose
690 mixture with either 0 μM (Control), 30 μM, 100 μM, 300 μM, 1 mM, 3 mM, or 10 mM glyphosate.
691 The cotton balls were replaced every third day with new cotton balls and fresh
692 sucrose/glyphosate solutions. Mosquito death was monitored daily for 14 days. Experiments
693 were performed in three independent replicates, for a total of 120 mosquitoes in each treatment
694 group.

695 ***Anopheles gambiae* Cuticle Pigmentation and Wing Size**

696 Adult female mosquitoes were drugged for 5 days as previously described. Mosquitoes
697 were cold euthanized and mounted dorsally on a slide with double-sided tape. Images of the
698 mosquito ventral abdomen were taken under a dissection microscope with constant exposure
699 and lighting conditions. Pigmentation was measured using Fiji software (133). The entire
700 abdomen of each mosquito was selected using a freehand selection tool, and the 8-bit mean
701 gray value was measured using the Measure tool. A measurement of 0 corresponds to a pure
702 black gray value, whereas 255 corresponds to a pure white gray value.

703 Following abdomen pigmentation measurements, mosquito bodies were removed, with
704 careful attention to keeping the wings remaining intact on the tape. Intact wings were imaged on
705 a microscope, and the length of the individual wing lengths were measured from tip-to-tip using
706 Fiji Measure tool.

707 ***Anopheles gambiae* infection with *Plasmodium falciparum***

708 Adult female mosquitoes (3-4 d old) of *A. gambiae* Keele strain were sorted and drugged
709 as described above. On the fifth day of glyphosate exposure, mosquitoes were provided a blood
710 meal containing *P. falciparum.* Blood-fed engorged mosquitoes were sorted on ice and fed 10%
711 sucrose *ad libitum* for 8 d. Midguts were dissected and stained with 0.2% Mercurochrome

712 solution and oocysts were enumerated using a 20X objective with light microscopy. See
713 Supplementary Fig. 9b.

714 ***Anopheles gambiae* Midgut Microbiome Analysis**

715 Adult female mosquitoes (3-4 d old) of *A. gambiae* Keele strain were sorted and drugged
716 as described above. On the fifth day of glyphosate exposure, mosquitoes were sterilized in
717 ethanol for 2 minutes, washed, and dissected in sterile PBS. The midguts were removed, placed
718 in 500 µl sterile PBS on ice, homogenized, diluted, and plated on LB agar plates. Plates were
719 incubated at 30°C for three days and individual colonies were counted. Each experiment used
720 10-20 mosquitoes per condition, and the experiment was performed three independent times.

721 For the 16S rRNA sequencing studies, mosquitoes were reared, drugged, and then
722 midguts were dissected as described above, with five individual midguts per condition. DNA was
723 extracted from frozen mosquito samples using the Lucigen EpiCentre MasterPure DNA
724 extraction kit. The bacterial 16S rRNA gene was amplified by PCR, and sample-specific Illumina
725 adapters were ligated to the PCR products. PCR products from multiple samples were pooled
726 and sequenced on the Illumina MiSeq platform by the University of Connecticut MARS Facility.
727 Data were then analyzed using mothur (136) to construct contigs to align forward and reverse
728 reads, remove ambiguous bases and chimeric regions, align sequences to the Silva 16S V4
729 reference database, and cluster reads into 3% operational taxonomic units (OTUs). Sequences
730 derived from known contaminants were selectively removed. Alpha and beta diversity
731 measurements were performed using the Shannon diversity index and Bray-Curtis dissimilarity
732 distance respectively. Bray-Curtis distances were graphed on principal coordinates analysis
733 (PCoA) plots in two dimensions. Taxa and PCoA graphs were produced using
734 MicrobiomeAnalyst (137,138). See Supplementary Fig. 9c.

735 **Dopaquinone Formation MBTH Assay**

736 Quinones like dopaquinone are unstable and difficult to study directly; thus,
737 dopaquinone quantification relies on the formation of a stable adduct with MBTH (3-methyl-2-

benxothiaxolinone hydrazine) that forms a pigment that absorbs at 505 nm(139). This absorption overlaps with the absorption of another melanin intermediate, dopachrome (Q), but is not expected to interfere since dopaquinone reaction with MBTH prevents dopachrome formation. Further, the molar absorbance coefficient for MBTH-Dopaquinone is more than 10 times higher (39,000 L/[mol cm]) than that of dopachrome (3,700 L/[mol cm]), and interference from dopachrome would be relatively small.

MBTH reaction mixtures were prepared as previously described (139). This mixture is warmed at 42°C to help solubilize the components. Then, 5 µl of 2 µg/ml Mushroom Tyrosinase (Sigma, Product #T382) and 20 µl of 20 mM L-DOPA are added to the MBTH solution, and 160 µl of the solution is immediately added to each well containing compounds. The plate was read at an absorbance of 505 nm for 30 min at 30°C, and read again at 1 h and overnight. The dopaquinone levels are determined by the formation of the bright pink adduct between the quinone and the MBTH.

Dopachrome and Melanin Measurements

Tyrosinase activity was determined as previously described (135), substituting mushroom tyrosinase for phenoloxidase. The formation rate of dopachrome is measured as the maximum velocity of this reaction, and the dopachrome levels are measured as the absorbance at 490 nm after 30 min as the absorbance values plateau. Melanin levels are measured as the absorbance at 490 nm after the reaction has continued for 5 d in the dark at room temperature.

Free-Radical Scavenging ABTS Assay

ABTS solution was prepared as previously described (140). To test the radical-scavenging capability of the compounds, 10 µl of the compounds were serially diluted in a 96 well plate as previously described, and 90 µl of diluted ABTS was added to each well. The 734 nm absorbance was measured immediately, after 10 min, 1 and 2 h. In kinetics experiments, absorbance readings were taken every two minutes for 5 h.

To measure the radical scavenging capacity of the synergistic compounds and L-DOPA mixtures, ABTS was prepared and diluted in Milli-Q water. In each well, 5 µl of compound stocks were added with either 5 µl of water or 5 µl of 500 µM L-DOPA. Next, 90 µl of ABTS solution was added to the well, and the absorbance was read immediately at 734 nm. Synergy was calculated from this data using the following formula:

$$\text{Synergy Ratio} = \frac{(\Delta\text{Abs 734 Compound Alone} + \Delta\text{Abs 734 DOPA Alone})}{\Delta\text{Abs 734 Compound with DOPA}}$$

Glyphosate Effect on L-DOPA

To determine if L-DOPA is reacting with glyphosate, we analyzed by NMR. We diluted 300 mM stock of glyphosate in water to 60 mM (10 mg/ml) in D_2O, prepared 20 mM (4 mg/ml) L-DOPA in D_2O, and prepared two mixtures of glyphosate and L-DOPA: one with 20 mM (4 mg/ml) L-DOPA and 60 mM (10 mg/ml) of glyphosate in D_2O, and another with a low concentration of 1 mg/ml for both compounds equaling 5 mM L-DOPA and 6 mM glyphosate. We then performed ^{31}P-NMR and ^{1}H-NMR on these samples.

Glyphosate Effect on Tyrosinase

To determine the tyrosinase kinetics with glyphosate as an inhibitor, we serially diluted 155 µl of 20 mM L-DOPA in Milli-Q water. To each dilution of L-DOPA we added 20 µl of glyphosate diluted in PBS and 5 µl of 2 µg/ml mushroom tyrosinase to the reaction mix. In order to account for non-enzymatic oxidation of L-DOPA, we ran an experiment in parallel, in which we added 5 µl of Milli-Q water instead of tyrosinase. The reaction mix was kept at 30°C for 24 h. The plate was read at 490 nm. To calculate enzyme-specific oxidation of L-DOPA, the no enzyme values were subtracted from the tyrosinase rows. The kinetics curve is plotted as a function of absorbance after 24 h of reaction time versus concentration of L-DOPA.

We tested if tyrosinase concentration had an effect on the percent inhibition of the reaction. We prepared dilutions of tyrosinase. We added 5 µl of each dilution to a 96-well plate, and added 135 µl of Milli-Q water, 20 µl of 20 mM L-DOPA, and 20 µl of glyphosate in PBS. We

788 measured maximum velocity of this reaction at 490 nm. The difference in velocities and percent
789 inhibition reported were calculated by difference = $V_{max\ water}$ - $V_{max\ glyph}$, and percent inhibition =
790 100*($V_{max\ glyph}$/$V_{max\ water}$).

791 To determine if glyphosate irreversibly affects tyrosinase activity, 450 µl of 20 µg/ml
792 mushroom tyrosinase was prepared in 450 µl of 50 mM sodium phosphate buffer, pH 7, either
793 with 50 µl of 300 mM glyphosate, or 50 µl of Milli-Q water. The enzyme solution was loaded into
794 a hydrated 10,000 MWCO Slide-a-lyzer dialysis cassette (Thermo Scientific), and the enzyme
795 solutions were dialyzed in a 50 mM sodium phosphate buffer at 4°C, according to the
796 manufacturer's protocol. Protein concentrations were measured and normalized using sodium
797 phosphate buffer. To measure the kinetics of the control enzyme versus the treated enzyme, a
798 kinetics assay was performed as previously described. Each reaction's maximum velocity is
799 determined and plotted.

800 **Copper Rescue of Melanin Inhibition**

801 As previously described, serial dilutions of glyphosate were arrayed in eight rows; one
802 row per copper ion concentrations to be tested. Copper sulfate was prepared and serially diluted
803 and 10 µL of the copper solution is added to each well containing the glyphosate dilution. To
804 each well 150 µL of reaction mix (125 µL of Milli-Q water, 20 µL of 20 mM L-DOPA, and 5 µL of
805 2 µg/mL mushroom tyrosinase (5 µl of water used for auto-oxidation experiments) was added.
806 The final copper ion concentrations were 400, 200, 100, 50, 25, 12.5, 6.25, and 0 µM. The
807 dopachrome and melanin measurements are reported as previously described.

808 **Cyclic Voltammetry**

809 Cyclic voltammetry was performed using a Metrohm Autolab potentiostat (Switzerland),
810 3 mm Glassy Carbon working electrode, 10 mm x 10 mm x 0.1 mm platinum plate counter
811 electrode, and an Ag/AgCl reference electrode in 3 M KCl solution. Solutions were prepared in
812 0.1x PBS (Difco) at a pH 6.00, adjusted with NaOH and HCl. 10 mL of L-DOPA solution was
813 freshly prepared in this buffer, and 1 mL of glyphosate, glycine, water, etc, solution at pH 6.00

814 were added to the L-DOPA. Readings were done with three tracings at a scan rate of 50 mV/s
815 at intervals of 5 mV steps. Glassy carbon electrode was washed and polished between readings
816 with slurry of alumina powder and water on cloth pads.
817
818 **DATA AVAILABILITY**
819 The 16S rRNA sequencing datasets generated during this study are available at Mendeley Data
820 at DOI:10.17632/6ymh76hmzm.1, and the datasets from the remaining experiments are
821 available at Mendeley Data at DOI: 10.17632/xndcmbn6wd.2.
822
823 **FIGURE LEGENDS**
824 **Fig. 1.** ***Glyphosate Inhibits G. mellonella Melanization and Increases Infection***
825 ***Susceptibility.*** **(A**) Glyphosate inhibits the phenoloxidase activity of 1:10 dilutions of
826 hemolymph without exogenously added L-DOPA. (**B**) AMPA, a primary metabolite of
827 glyphosate, inhibits *G. mellonella* phenoloxidase-mediated melanization similar to glyphosate.
828 Error bars in **(A-B)** represent ± SD (**C**) *G. mellonella* larvae drugged with glyphosate solution
829 (10 µl of 1 mM) in PBS and infected 5 h post treatment with 10^4 cells of WT *C. neoformans* die
830 rapidly compared to PBS-treated controls. Death events were recorded daily. Each infection
831 condition represents survival of 95 animals, pooled together from four biological replicates, and
832 six total technical replicates. Statistical significance was assessed by Gehan-Breslow-Wilcoxon
833 test, which we used to place weight on early timepoints in the survival curve. We used this test
834 because we expected to see the glyphosate-mediated differences early in the infection due to
835 the timing of the glyphosate treatment. Since w where the expected effects of the one-time pre-
836 treatment with glyphosate would be. **(D)** The size of the dark melanized particles within nodules
837 upon *C. neoformans* infection are significantly smaller in the glyphosate-treated (10 µl of 1 mM)
838 infected groups compared to the PBS-treated infected groups, which were analyzed for
839 significance using a nested non-parametric Mann-Whitney-Wilcoxon rank test. Horizontal bar

represents the median value and the error bars represent the 95% Confidence Interval **(E)** The degree of melanin encapsulation of the yeast within the nodule is also reduced in the glyphosate-treated (10 µl of 1 mM) groups, as measured on a scale of 0 (no melanin encapsulation) to 4 (very high levels of melanin encapsulation) as demonstrated in (**F**). Numbers in each bar represent the number of encapsulated *C. neoformans* for each score. Statistical significance was assessed using a Chi-squared table test. Data in (**D**) and (**E)** represent data over three independent replicates with three larvae used per condition per replicate. (**G**) Representative brightfield micrographs showing the hemocyte and nodule formation in the different treatment groups at 20x and 100x magnification. Scale bars represent 10 µm. Nested non-parametric Mann-Whitney-Wilcoxon rank test performed using R for R 4.0.2 GUI 1.72 for Mac OS at https://www.r-project.org/ (R Core Team, 2020) and the *nestedRanksTest* package (*Version 0.2*, D.G. Scofield , 2014)(134). All other statistical analyses performed using GraphPad Prism version 8.4.3 for Mac OS, GraphPad Software, San Diego California USA, www.graphpad.com. See also, Supplementary Fig. 1.

Fig. 2. *Glyphosate Effects on A. gambiae Phenoloxidase Activity and Susceptibility to Plasmodium Infection*. (**A**) Glyphosate inhibits phenoloxidase activity in *A. gambiae* homogenate. Enzyme activity represents three biological replicates with three technical replicates for each condition. (**B)** Glyphosate treatment increases the susceptibility of the *A. gambiae* to *P. falciparum* infection as measured by oocyst count per midgut. Increased glyphosate doses are associated with increased median oocyst burden. Parasite infection represents four biological replicates and four separate infections, line indicates median, and differences in parasite burden analyzed for significance using non-parametric Kruskal–Wallis test with each group compared to the control group with Dunn's correction for multiple comparisons. **(C)** Low doses of glyphosate enhance the survival of adult mosquitoes, while the higher doses diminish their survival as compared to the control. Survival curves represent 120 animals from three independent replicates composed of

groups of 40 mosquitoes, and survival was examined for statistical significance using the Log-Rank Mantel-Cox analysis with a Bonferoni correction for multiple comparisons. (D) Hazard ratios calculated from the Cox Mixed Effects Model to account for fixed (glyphosate treatment) and random effects (replicate). Hazard ratios<1 indicate lower risk of death compared to control values, and values >1 indicate a higher risk of death compared to the control. Hazard Ratio of 1 is depicted by a dotted line. The Cox Mixed Effects modeling was performed using R for R 4.0.2 GUI 1.72 for Mac OS at https://www.r-project.org/ (R Core Team, 2020) and the *coxme* package (*Version 2.2-16*, T.M. Therneau, 2020)(141). All other statistical analyses performed using GraphPad Prism version 8.4.3 for Mac OS, GraphPad Software, San Diego California USA, www.graphpad.com. The statistical significance in **(C)** is coded as: ns - p > 0.05, * - p<0.05, ** - p<0.01, *** -p<0.001, and **** - p<0.0001. See also Supplementary Fig. 2.

Fig. 3. ***Glyphosate Alters the Composition, but Not Density, of the A. gambiae Midgut Microbiota.*** (**A**) Glyphosate does not alter microbial density of the culturable mosquito midgut bacteria (grown on LB agar). Each sample consists of 40-50 individual mosquito midguts over three independent replicates. Error bars represent the mean and ±SD. **(B)** Glyphosate alters the composition of the mosquito microbiota, leading to decrease of Entereobacteriacae and an increase of *Asaia* spp. **(C)** The glyphosate treatments do not significantly alter alpha diversity as measured by the Shannon Index (statistical analysis conducted using one-way ANOVA; NS = p >0.05). **(D)** However, the glyphosate-treated and control-treated microbiota form distinct clusters in principle coordinates analysis, measured by Bray-Curtis dissimilarity. Statistical significance was tested by PERMANOVA (p <0.001, R=0.557). Each treatment group represents 5 individual mosquito midguts. For more information see also Supplementary Fig. 3.

Fig. 4. ***Glyphosate Inhibits in vitro Melanin Production.*** **(A)** An overall schematic of the Mason-Raper pathway of melanization mediated by tyrosinase and auto-oxidation. (**B)**

892 Glyphosate inhibits formation of dopaquinone produced by tyrosinase-mediated and
893 spontaneous oxidation of L-DOPA. Dopaquinone is indicated by the absorbance of an MBTH-
894 Dopaquinone adduct pigment at 505 nm. Absorption levels are shown relative to the no
895 glyphosate control with background (MBTH mixture) subtracted after 1 h at 30ºC **(C)** Glyphosate
896 decreases the rate of dopachrome formation and inhibits dopachrome production from
897 tyrosinase oxidation of L-DOPA. Rate of dopachrome formation is the reaction V_{max} at 490 nm
898 relative to the V_{max} without glyphosate. Dopachrome production is shown as the absorbance at
899 490 nm relative to the control after 30 min of reaction. **(D)** Melanin production is inhibited by
900 glyphosate with tyrosinase and auto-oxidation of L-DOPA. Melanin levels are measured as the
901 absorbance at 490 nm after 5 d of reaction. Inset shows a representative image of the data in
902 (**D**) showing melanization inhibition with increasing glyphosate concentration. Values are
903 depicted relative to the no glyphosate control. Error bars represent ±SD. Each experiment was
904 performed at least three independent replicates.
905
906 **Fig. 5.** ***Phosphate-Containing Compounds Inhibited Melanization Similarly to Glyphosate.***
907 Glyphosate, *o*-phosphoserine (PS), phosphonoacetic acid (PAA), pyrophosphate (pyro), and
908 phosphoric acid (PA) inhibit dopaquinone formation **(A)**, rate of dopachrome formation **(B)** and
909 dopachrome levels **(C)**, and melanin formation **(D)**, whereas their respective non-phosphate
910 analogs, glycine (gly), serine (ser), and acetic acid (AA) do not inhibit any step of melanization
911 **(A-D)**. (**E)** Auto-oxidation of L-DOPA is inhibited by glyphosate, PS, PAA, Pyro, and PA in a
912 similar manner. The compounds tested (**F)** were diluted in 300 mM stock solution and titrated to
913 pH between 5 and 6. Absorption and rates are shown relative to the internal no drug control.
914 Grayscale bars represent mean absorbance at 490 nm relative to no compound control. The
915 darker colors correspond to increased pigment formation. Inset shows a representative image of
916 the data in (**E**) showing the effects of the compounds on auto-oxidation. Error bars in (**A-C)**
917 represent ±SD. Each experiment represents at least three independent replicates.

Fig. 6. ***Glyphosate Does Not Directly Inhibit Tyrosinase Activity*** **(A).** Tyrosinase activity is not irreversibly inhibited and glyphosate-treated enzyme has normal activity when glyphosate is dialyzed out of solution. **(B)**. Glyphosate appears as a non-competitive inhibitor of tyrosinase in Michaelis-Menten kinetics assays measuring the change in absorbance at 490 nm over 24 h compared to the no tyrosinase background. **(C)** The rate of dopachrome formation with glyphosate treatment is smaller than the slope of the control treatment across all concentrations of tyrosinase. This reduced slope indicates reversible inhibition. The assay is performed under constant L-DOPA and glyphosate concentrations. Shaded areas represent the 95% CI of the linear regression **(D)** Adding Cu^{+2} to L-DOPA-tyrosinase reactions with glyphosate does not rescue melanin inhibition compared to the glyphosate-free control. (See also Supplementary Fig. 5) Grayscale bars represent mean absorbance at 490 nm relative to no glyphosate and no copper control. The darker colors correspond to increased pigment formation. Error bars in **(A-C)** represent ±SD. Each experiment represents at least three independent replicates.

Fig. 7. ***Glyphosate Affects the Oxidative Properties of Melanogenesis.*** (**A)** None of the melanin inhibitors exhibit radical quenching properties in an ABTS assay aside from glyphosate, which shows weak antioxidant properties after several hours in the ABTS solution. Absorbance at 734 nm is an indicator of how much ABTS remains in radical form (not quenched). (**B-C)** Citric acid (CA), a non-radical quenching antioxidant (antioxidant synergist) exhibits similar melanin inhibition as glyphosate and phosphoric acid, another known antioxidant synergist. Grayscale bars in **(C)** represent absorbance at 490 nm relative to no compound control, with the darker colors correspond to increased pigment formation**. (D)** Glyphosate, phosphoserine, phosphoric acid, and citric acid show synergy with the antioxidant L-DOPA. The addition of these compounds to L-DOPA enhances its radical quenching abilities by approximately 50%. Black dotted line represents the normalized ABTS absorbance treated with water. The other compounds tested here alone do not

show much deviation from this line. The blue dotted line indicates the ABTS solution treated with L-DOPA alone. ABTS treated with L-DOPA and synergetic compounds together are below this line. (**E)** Average cyclic voltammogram showing the changes in oxidation and reduction of L-DOPA and dopaquinone when exposed to 16 mM glyphosate but not water. Numbers correspond to shifted peaks or peaks with less current compared to the water control. Peak 1 corresponds to L-DOPA oxidation (**F**); Peak 2 likely corresponds to dopaquinone reduction (**G**). glyphosate shifts Peak 1 and 2 toward a decreased redox potential and diminishes the current of Peak 1 and 2 in a dose-dependent manner (**H**) - notably decreasing Peak 2 current intensity to the point of non-existence **(I)**. Each experiment represents at least three independent replicates. Error bars in (**A-B, D**) represent ±SD. See also Supplementary Fig. 6 and 8 .

Supplementary Fig. 1. *G. mellonella* Supplemental Data. (A) Broad-spectrum protease inhibitor (cOmplete, Roche) was added to *G. mellonella* hemolymph to prevent the activation of new phenoloxidase, and to control for any impact that glyphosate may have on phenoloxidase activation cascade, cell viability, and gene expression. The general trend remains the same that glyphosate inhibits phenoloxidase activity with and without protease inhibitor, albeit lower with protease inhibitor due to the lower concentration of activated enzyme. **(B)** Phenoloxidase activity was assessed using exogenous L-DOPA for one batch of *G. mellonella,* during these experiments, the lower concentration of glyphosate resulted in increased phenoloxidase activity as compared to the control. This suggests that there may be some cellular regulation of phenoloxidase induced by glyphosate. It is possible that the doses of glyphosate tested elicit some cellular response that increases phenoloxidase expression, secretion, and/or activation as a feedback/hormesis-like response to the reduced melanin production. These data represent three independent replicates, but this pattern of enzymatic activity as a function of glyphosate concentration was not seen in subsequent batches of larvae. (**C)** Hemocyte viability was not dramatically affected by concentrations of glyphosate ranging from 100 µM to 10 mM, indicating

that our data are likely not artifacts of cytotoxic concentrations of glyphosate. Error bars in **(A-C)** represent ± SD. (**D)** AMPA, a major metabolite of glyphosate, inhibits tyrosinase-mediated melanization similar to glyphosate. Grayscale bars represent mean absorbance at 490 nm relative to no compound control. The darker colors correspond to increased pigment formation. **(E)** Larvae treated with glyphosate and subsequently infected with *lac1Δ* mutant *C. neoformans* strain showed a similar pattern of increased susceptibility as the wild type H99, although the differences in susceptibility with the *lac1Δ* infected larvae are not statistically significant. Each experiment represents at least three independent replicates. The PBS mock infection condition represents survival of 95 animals, over the span of four biological replicates, and six total technical replicates. The *lac1Δ* mutant infection represents survival of 75 animals over the span of four biological replicates. The PBS mock infection data is the same as the data in Fig. 5b, as all the infections were done concurrently under the same conditions. (**F)** Single injection of 10 µl of 1mM glyphosate does not affect the pupation of *G. mellonella* at 30°C and room temperature (RT). Data from 30°C represents 25-35 animals for each group over two biological replicates, and data from RT represents 45 animals from each group over three biological replicates. Statistical analysis performed using Log-rank Mantel-Cox tests. (**G-I**) The three individual replicates from **Fig. 1D** showing the size of the dark melanized particles within nodules are significantly smaller in the glyphosate-treated infected groups compared to the PBS-treated infected groups, with (**G**) and **(H)** showing that there were more melanized spots in the PBS-treated infected group compared to the glyphosate-treated. All statistical analyses performed using GraphPad Prism version 8.4.3 for Mac OS, GraphPad Software, San Diego California USA, www.graphpad.com.

Supplementary Fig. 2 Low efficiency *Plasmodium falciparum* infection of *A. gambiae and effects on mosquito cuticle* (**A**). Oocyst count per midgut for mosquitoes treated with or without glyphosate and infected with high-passage *Plasmodium falciparum* gametocyte culture,

resulting in a low efficiency infection. Data represents one biological replicate. Dotted black line indicates y=0. Black lines for each condition indicate median oocyst count per midgut. We have chosen not to include the data from this replicate in the data shown in Fig. 6, because the results from this one-off replicate appear due to poorly infectious parasite culture. Additionally, it is difficult to make comparisons using the low infection burden of the control group with a with the treatment groups, as well other replicates with higher oocyst burdens. **(B)** Infection prevalence (percent midguts with at least one oocyst) from the experiment described in (**A**). Fisher's Exact test performed for each condition individually compared to control and corrected for multiple comparisons using the Bonferroni method. **(C)** 5 days of 1 mM glyphosate treatment in adult female mosquitoes does not influence the abdomen's cuticular darkness as measured by mean gray value with 0 being pure black and 255 being pure white. Data representative of 2 biological replicates with 88 mosquitoes measured per condition. **(D)** Wing length, as a proxy for body mass and size, is not affected by 5 days of glyphosate treatment. Data representative of a single biological replicates with 32-36 mosquitoes measured per condition. Line and error bar represent mean ± SD in **(C-D).** Unpaired t-test performed to determine statistical significance in **(C-D).** All statistical analyses performed using GraphPad Prism version 8.4.3 for Mac OS, GraphPad Software, San Diego California USA, www.graphpad.com.

Supplementary Fig. 3. ***Glyphosate affects the A. gambiae microbiota in a dose-independent manner*** **(A)** At the class level, glyphosate leads to an enrichment of Alphaproteobacteria and a depletion in Gammaproteobacteria**.** Tables showing the relative abundance of bacterial classes (**B)** and individual bacterial genera (**C**) following glyphosate treatment . (**D)** Alpha diversity does not follow a distinctive pattern with increasing glyphosate dose. **(E)** Glyphosate-treated and control-treated microbiota cluster separately in ordination space, but the clusters are not dose-dependent.

Supplementary Fig 4. ***Reaction of glyphosate with L-DOPA.*** Representative ^{1}H NMR spectra of 60 mM glyphosate solution in D_2O (**Green**), 20 mM L-DOPA solution in D_2O (**Red)**, and 20 mM L-DOPA mixed with 60 mM glyphosate in D_2O (**Blue**). There appears to be no shift in ^{1}H peaks and no appearance of new peaks, which is indicative of no reaction occurring between the compounds. Data representative of three independent replicates

Supplementary Fig. 5. ***Glyphosate appears to "buffer" copper concentration in solution*****.** High doses (2-16 mM) of glyphosate prevent the enzymatic activity enhancing effects of lower copper concentration (6.25-25 μM), but high doses of glyphosate also prevent the enzyme inhibitory effects of high copper concentration (100-400 μM)**.** Error bars represent ±SD. Data represents at least three independent replicates.

Supplementary Fig. 6. ***Antioxidant Properties of glyphosate.*** **(A)** Change in absorbance of ABTS solution at 734 nm over time for 33.33 mM glyphosate relative to the no glyphosate control. This indicates glyphosate quenches free radicals over an extended period of time. **(B**) Calculated antioxidant radical scavenging synergy between compounds tested and L-DOPA. Values represent the mean of at least three independent replicates. Error bars represent ±SD.

Supplementary Fig. 7. ***Glyphosate inhibits melanin production independent of L-DOPA concentration.*** (**A)** Inhibitory concentrations of glyphosate are not affected by L-DOPA concentration. This indicates that glyphosate is not reacting proportionately with L-DOPA as measured by absorbance at 490 nm after 5 d of reaction, relative to the no glyphosate control and with background absorbance subtracted. (**B**) The IC_{50} of glyphosate remains constant at approximately 1 mM relative inhibition of melanin production appears dependent on glyphosate concentration alone, and not on L-DOPA to glyphosate ratio. Error bars represent ±SD. Each experiment represents at least three independent replicates. Grayscale bars represent mean

absorbance at 490 nm relative to no compound control. The darker colors correspond to increased pigment formation. Red line represents the approximate IC_{50}. Crossed out boxes represent values with no data.

Supplementary Fig. 8. Cyclic Voltammetry Supplemental Data. (A) Peak 1 was validated as the oxidation of L-DOPA, and Peak 2 was validated as the reduction peak of dopaquinone by correlating increased peak intensity with increasing concentration of L-DOPA under the same potentiostat parameters. **(B)** Glycine (16 mM) – a non-phosphate analog of glyphosate, a non-inhibitor of melanization, and a non-antioxidant - does not alter the oxidation potential of L-DOPA. Conversely, Citric Acid (16 mM) – a known synergistic antioxidant and inhibitor of melanization – does alter the oxidation potential of L-DOPA in similar ways as glyphosate. Each experiment represents at least three independent replicates, with three cycles per replicate. The tracings represent the mean value of the three replicates over the course of three cycles.

Supplementary Fig. 9. Experimental Methods Diagram for Insect Experiments. (A). During *G. mellonella* infection with *C. neoformans,* larvae were injected with 10 µl of 1 mM glyphosate, left to recover for 5 h, and were subsequently infected with 10^4 cells/larvae of *C. neoformans* H99 strain. Survival was monitored for 14 days. (**B**) During *A. gambiae* infection with *P. falciparum,* mosquitoes were drugged with glyphosate-laced 10% sucrose solution for 5 days, then fed with a *P. falciparum*-infected blood meal, and fed 10% sucrose for 8 d. On Day 8, mosquitoes were dissected, and the midguts were stained with mercurochrome to facilitate oocyst enumeration. **(C)** glyphosate-drugged mosquitoes were dissected under sterile conditions, and five midguts were collected individually per condition. DNA was extracted from samples and bacterial 16S rRNA genes were amplified by PCR and sample-specific Illumina adapters were ligated to products. PCR products were pooled and sequenced on the Illumina MiSeq platform. Data were then analyzed using mothur to construct contigs, align reads, remove ambiguous bases and chimeric regions, align sequences to the Silva

16S V4 reference database, and cluster reads into 3% operational taxonomic units (OTUs). Sequences from known contaminants were removed. Alpha and beta diversity measurements were performed using the Shannon diversity index and Bray-Curtis dissimilarity distance respectively and plotted using MicrobiomeAnalyst. Figures made with BioRender.

REFERENCES:

1. Whitten MMA, Coates CJ. Re-evaluation of insect melanogenesis research: Views from the dark side. Pigment Cell & Melanoma Research. 2017;30(4):386–401.

2. Prota G. Recent Advances in the Chemistry of Melanogenesis in Mammals. Journal of Investigative Dermatology. 1980 Jul 1;75(1):122–7.

3. Nappi AJ, Christensen BM. Melanogenesis and associated cytotoxic reactions: Applications to insect innate immunity. Insect Biochemistry and Molecular Biology. 2005 May 1;35(5):443–59.

4. Fujieda N, Murata M, Yabuta S, Ikeda T, Shimokawa C, Nakamura Y, et al. Multifunctions of MelB, a Fungal Tyrosinase from Aspergillus oryzae. ChemBioChem. 2012;13(2):193–201.

5. Lerch K. Tyrosinase: Molecular and Active-Site Structure. In: Enzymatic Browning and Its Prevention [Internet]. American Chemical Society; 1995 [cited 2020 Oct 21]. p. 64–80. (ACS Symposium Series; vol. 600). Available from: https://doi.org/10.1021/bk-1995-0600.ch005

6. Galván I, Solano F. Bird Integumentary Melanins: Biosynthesis, Forms, Function and Evolution. International Journal of Molecular Sciences. 2016 Apr;17(4):520.

7. Martín-Durán JM, de Mendoza A, Sebé-Pedrós A, Ruiz-Trillo I, Hejnol A. A Broad Genomic Survey Reveals Multiple Origins and Frequent Losses in the Evolution of Respiratory Hemerythrins and Hemocyanins. Genome Biol Evol. 2013 Jul 1;5(7):1435–42.

8. Ramsden CA, Riley PA. Tyrosinase: The four oxidation states of the active site and their relevance to enzymatic activation, oxidation and inactivation. Bioorganic & Medicinal Chemistry. 2014 Apr 15;22(8):2388–95.

9. Christensen BM, Li J, Chen C-C, Nappi AJ. Melanization immune responses in mosquito vectors. Trends in Parasitology. 2005 Apr 1;21(4):192–9.

10. González-Santoyo I, Córdoba-Aguilar A. Phenoloxidase: a key component of the insect immune system. Entomologia Experimentalis et Applicata. 2012;142(1):1–16.

11. Marmaras VJ, Charalambidis ND, Zervas CG. Immune response in insects: the role of phenoloxidase in defense reactions in relation to melanization and sclerotization. Arch Insect Biochem Physiol. 1996;31(2):119–33.

12. Chen CC, Chen CS. Brugia bahangi: Effects of Melanization on the Uptake of Nutrients by Microfilariae in Vitro. Experimental Parasitology. 1995 Aug 1;81(1):72–8.

13. Zhao P, Lu Z, Strand MR, Jiang H. Antiviral, anti-parasitic, and cytotoxic effects of 5,6-dihydroxyindole (DHI), a reactive compound generated by phenoloxidase during insect immune response. Insect Biochem Mol Biol. 2011 Sep;41(9):645–52.

14. Ezzati-Tabizi R, Talaei-Hassanloui R, Farrokhi N, Hossininaveh V, Alavi M. Haemolymph phenoloxidase activity of larval Plodia interpunctella and Galleria mellonella in response to Beauveria bassiana and Pseudomonas fluorescens. International Journal of Agriculture Innovations and Research. 2013;2(2):217–20.

15. Vertyporokh L, Hułas-Stasiak M, Wojda I. Host–pathogen interaction after infection of Galleria mellonella with the filamentous fungus Beauveria bassiana. Insect Science. 2020;27(5):1079–89.

16. Nayar JK (University of F, Knight JW. Wounding increases intracellular encapsulation (melanization) of developing Brugia malayi (Nematoda: Filarioidea) larvae in thoracic muscles of Anopheles quadrimaculatus. Comparative biochemistry and physiology Part A, Physiology (USA) [Internet]. 1995 [cited 2020 Oct 21]; Available from: https://agris.fao.org/agris-search/search.do?recordID=US9619494

17. Nayar JK, Knight JW, Vickery AC. Intracellular Melanization in the Mosquito Anopheles quadrimaculatus (Diptera: Culicidae) Against the Filarial Nematodes, Brugia spp. (Nematoda: Filarioidea). J Med Entomol. 1989 May 1;26(3):159–66.

18. Yassine H, Kamareddine L, Osta MA. The Mosquito Melanization Response Is Implicated in Defense against the Entomopathogenic Fungus Beauveria bassiana. PLOS Pathogens. 2012 Nov 15;8(11):e1003029.

19. Zdybicka-Barabas A, Cytryńska M. Phenoloxidase activity in hemolymph of Galleria mellonella larvae challenged with Aspergillus oryzae. 2011 [cited 2020 Oct 21]; Available from: https://pubag.nal.usda.gov/catalog/5208902

20. Dimopoulos G, Müller H-M, Levashina EA, Kafatos FC. Innate immune defense against malaria infection in the mosquito. Current Opinion in Immunology. 2001 Feb 1;13(1):79–88.

21. Schnitger AKD, Kafatos FC, Osta MA. The Melanization Reaction Is Not Required for Survival of Anopheles gambiae Mosquitoes after Bacterial Infections. J Biol Chem. 2007 Jul 27;282(30):21884–8.

1142 22. Dubovskiy IM, Kryukova NA, Glupov VV, Ratcliffe NA. Encapsulation and nodulation in
1143 insects. Invertebrate Survival Journal. 2016 Jul 7;13(1):229–46.

1144 23. Du M-H, Yan Z-W, Hao Y-J, Yan Z-T, Si F-L, Chen B, et al. Suppression of Laccase 2
1145 severely impairs cuticle tanning and pathogen resistance during the pupal
1146 metamorphosis of Anopheles sinensis (Diptera: Culicidae). Parasites Vectors. 2017
1147 Apr 4;10(1):171.

1148 24. Qiao L, Du M, Liang X, Hao Y, He X, Si F, et al. Tyrosine Hydroxylase is crucial for
1149 maintaining pupal tanning and immunity in Anopheles sinensis. Scientific Reports.
1150 2016 Jul 15;6(1):29835.

1151 25. Goulson D. The insect apocalypse, and why it matters. Current Biology. 2019 Oct
1152 7;29(19):R967–71.

1153 26. Nosanchuk JD, Ovalle R, Casadevall A. Glyphosate Inhibits Melanization of Cryptococcus
1154 neoformans and Prolongs Survival of Mice after Systemic Infection. J Infect Dis. 2001
1155 Apr 1;183(7):1093–9.

1156 27. Samsel A, Seneff S. Glyphosate pathways to modern diseases V: Amino acid analogue of
1157 glycine in diverse proteins. Journal of Biological Physics and Chemistry. 2016 Mar
1158 30;16(1):9–46.

1159 28. Duke SO, Powles SB. Glyphosate: a once-in-a-century herbicide. Pest Management
1160 Science. 2008;64(4):319–25.

1161 29. Dill GM. Glyphosate-resistant crops: history, status and future. Pest Management
1162 Science. 2008;61(3):219–24.

1163 30. Gianessi JC& L. Herbicide Tolerant Soybeans: Why Growers Are Adopting Roundup
1164 Ready Varieties [Internet]. 1999 [cited 2018 Jun 20]. Available from:
1165 http://agbioforum.org/v2n2/v2n2a02-carpenter.htm

1166 31. Benbrook CM. Impacts of genetically engineered crops on pesticide use in the U.S. -- the
1167 first sixteen years. Environ Sci Eur. 2012 Dec 1;24(1):24.

1168 32. Benbrook CM. Trends in glyphosate herbicide use in the United States and globally.
1169 Environ Sci Eur [Internet]. 2016 [cited 2018 Jun 20];28(1). Available from:
1170 https://www.ncbi.nlm.nih.gov/pmc/articles/PMC5044953/

1171 33. Bott S, Tesfamariam T, Candan H, Cakmak I, Römheld V, Neumann G. Glyphosate-
1172 induced impairment of plant growth and micronutrient status in glyphosate-resistant
1173 soybean (Glycine max L.). Plant Soil. 2008 Sep 11;312(1):185.

1174 34. Laitinen P, Rämö S, Siimes K. Glyphosate translocation from plants to soil – does this
1175 constitute a significant proportion of residues in soil? Plant Soil. 2007 Nov
1176 1;300(1):51–60.

1177 35. Singh S, Kumar V, Datta S, Wani AB, Dhanjal DS, Romero R, et al. Glyphosate uptake,
1178 translocation, resistance emergence in crops, analytical monitoring, toxicity and
1179 degradation: a review. Environ Chem Lett. 2020 May 1;18(3):663–702.

1180 36. Laitinen P, Siimes K, Rämö S, Jauhiainen L, Eronen L, Oinonen S, et al. Effects of Soil
1181 Phosphorus Status on Environmental Risk Assessment of Glyphosate and
1182 Glufosinate-Ammonium. Journal of Environmental Quality. 2008;37(3):830–8.

1183 37. Laitinen P, Rämö S, Nikunen U, Jauhiainen L, Siimes K, Turtola E. Glyphosate and
1184 phosphorus leaching and residues in boreal sandy soil. Plant Soil. 2009 Oct
1185 1;323(1):267–83.

1186 38. Lupi L, Bedmar F, Puricelli M, Marino D, Aparicio VC, Wunderlin D, et al. Glyphosate
1187 runoff and its occurrence in rainwater and subsurface soil in the nearby area of
1188 agricultural fields in Argentina. Chemosphere. 2019 Jun 1;225:906–14.

1189 39. Edwards WM, Triplett GB, Kramer RM. A Watershed Study of Glyphosate Transport in
1190 Runoff 1. Journal of Environmental Quality. 1980 12/01;9(4):661–5.

1191 40. Silva V, Montanarella L, Jones A, Fernández-Ugalde O, Mol HGJ, Ritsema CJ, et al.
1192 Distribution of glyphosate and aminomethylphosphonic acid (AMPA) in agricultural
1193 topsoils of the European Union. Science of The Total Environment. 2018 Apr
1194 15;621:1352–9.

1195 41. Battaglin WA, Meyer MT, Kuivila KM, Dietze JE. Glyphosate and Its Degradation Product
1196 AMPA Occur Frequently and Widely in U.S. Soils, Surface Water, Groundwater, and
1197 Precipitation. JAWRA Journal of the American Water Resources Association.
1198 2014;50(2):275–90.

1199 42. Bento CPM, Yang X, Gort G, Xue S, van Dam R, Zomer P, et al. Persistence of glyphosate
1200 and aminomethylphosphonic acid in loess soil under different combinations of
1201 temperature, soil moisture and light/darkness. Science of The Total Environment.
1202 2016 Dec 1;572:301–11.

1203 43. Yang X, Wang F, Bento CPM, Meng L, van Dam R, Mol H, et al. Decay characteristics and
1204 erosion-related transport of glyphosate in Chinese loess soil under field conditions.
1205 Science of The Total Environment. 2015 Oct 15;530–531:87–95.

1206 44. Laitinen P, Siimes K, Eronen L, Rämö S, Welling L, Oinonen S, et al. Fate of the herbicides
1207 glyphosate, glufosinate-ammonium, phenmedipham, ethofumesate and metamitron
1208 in two Finnish arable soils. Pest Management Science. 2006;62(6):473–91.

1209 45. Sviridov AV. Microbial degradation of glyphosate herbicides (Review). Applied
1210 biochemistry and microbiology. 2015 Mar;v. 51(2):188–95.

1211 46. Gill JPK, Sethi N, Mohan A, Datta S, Girdhar M. Glyphosate toxicity for animals. Environ
1212 Chem Lett. 2018 Jun 1;16(2):401–26.

1213 47. Druille M, Cabello MN, Omacini M, Golluscio RA. Glyphosate reduces spore viability and
1214 root colonization of arbuscular mycorrhizal fungi. Applied Soil Ecology. 2013 Feb
1215 1;64:99–103.

1216 48. Schafer JR, Hallett SG, Johnson WG. Rhizosphere Microbial Community Dynamics in
1217 Glyphosate-Treated Susceptible and Resistant Biotypes of Giant Ragweed (Ambrosia
1218 trifida). wees. 2014 Apr;62(2):370–81.

1219 49. Zobiole LHS, Kremer RJ, Oliveira RS, Constantin J. Glyphosate affects micro-organisms
1220 in rhizospheres of glyphosate-resistant soybeans. Journal of Applied Microbiology.
1221 2011;110(1):118–27.

1222 50. Van Bruggen AHC, He MM, Shin K, Mai V, Jeong KC, Finckh MR, et al. Environmental and
1223 health effects of the herbicide glyphosate. Science of The Total Environment. 2018
1224 Mar 1;616–617:255–68.

1225 51. Ratcliff AW, Busse MD, Shestak CJ. Changes in microbial community structure following
1226 herbicide (glyphosate) additions to forest soils. Applied Soil Ecology. 2006 Dec
1227 1;34(2):114–24.

1228 52. Busse MD, Ratcliff AW, Shestak CJ, Powers RF. Glyphosate toxicity and the effects of
1229 long-term vegetation control on soil microbial communities. Soil Biology and
1230 Biochemistry. 2001 Oct 1;33(12):1777–89.

1231 53. Weaver MA, Krutz LJ, Zablotowicz RM, Reddy KN. Effects of glyphosate on soil microbial
1232 communities and its mineralization in a Mississippi soil. Pest Management Science.
1233 2007;63(4):388–93.

1234 54. Pochron S, Simon L, Mirza A, Littleton A, Sahebzada F, Yudell M. Glyphosate but not
1235 Roundup harms earthworms (Eisenia fetida). Chemosphere. 2020 Feb 1;241:125017.

1236 55. Krams IA, Kecko S, Jõers P, Trakimas G, Elferts D, Krams R, et al. Microbiome symbionts
1237 and diet diversity incur costs on the immune system of insect larvae. Journal of
1238 Experimental Biology. 2017 Nov 15;220(22):4204–12.

1239 56. Lewis Z, Lizé A. Insect behaviour and the microbiome. Current Opinion in Insect
1240 Science. 2015 Jun 1;9:86–90.

1241 57. Weiss B, Aksoy S. Microbiome influences on insect host vector competence. Trends in
1242 Parasitology. 2011 Nov 1;27(11):514–22.

1243 58. Lesperance DN, Broderick NA. Microbiomes as modulators of Drosophila melanogaster
1244 homeostasis and disease. Current Opinion in Insect Science. 2020 Jun 1;39:84–90.

1245 59. Motta EVS, Raymann K, Moran NA. Glyphosate perturbs the gut microbiota of honey
1246 bees. Proc Natl Acad Sci USA. 2018 09;115(41):10305–10.

60. Blot N, Veillat L, Rouzé R, Delatte H. Glyphosate, but not its metabolite AMPA, alters the honeybee gut microbiota. PLOS ONE. 2019 Apr 16;14(4):e0215466.

61. Rio RVM, Jozwick AKS, Savage AF, Sabet A, Vigneron A, Wu Y, et al. Mutualist-Provisioned Resources Impact Vector Competency. mBio. 2019 Jun 25;10(3):e00018-19.

62. Haughton AJ, Bell JR, Wilcox A, Boatman ND. The effect of the herbicide glyphosate on non-target spiders: Part I. Direct effects on Lepthyphantes tenuis under laboratory conditions. Pest Management Science. 2001;57(11):1033–6.

63. Evans SC, Shaw EM, Rypstra AL. Exposure to a glyphosate-based herbicide affects agrobiont predatory arthropod behaviour and long-term survival. Ecotoxicology. 2010 Oct 1;19(7):1249–57.

64. Tahir HM, Basheer T, Ali S, Yaqoob R, Naseem S, Khan SY. Effect of Pesticides on Biological Control Potential of Neoscona theisi (Araneae: Araneidae). J Insect Sci [Internet]. 2019 Mar 1 [cited 2020 Oct 18];19(2). Available from: https://academic.oup.com/jinsectscience/article/19/2/17/5420491

65. Baglan H, Lazzari CR, Guerrieri FJ. Glyphosate impairs learning in Aedes aegypti mosquito larvae at field-realistic doses. Journal of Experimental Biology [Internet]. 2018 Oct 15 [cited 2020 Oct 14];221(20). Available from: https://jeb.biologists.org/content/221/20/jeb187518

66. Farina WM, Balbuena MS, Herbert LT, Mengoni Goñalons C, Vázquez DE. Effects of the Herbicide Glyphosate on Honey Bee Sensory and Cognitive Abilities: Individual Impairments with Implications for the Hive. Insects. 2019 Oct;10(10):354.

67. Tomé HVV, Schmehl DR, Wedde AE, Godoy RSM, Ravaiano SV, Guedes RNC, et al. Frequently encountered pesticides can cause multiple disorders in developing worker honey bees. Environmental Pollution. 2020 Jan 1;256:113420.

68. Cuhra M, Traavik T, Dando M, Primicerio R, Holderbaum DF, Bøhn T. Glyphosate-Residues in Roundup-Ready Soybean Impair Daphnia magna Life-Cycle. Journal of Agricultural Chemistry and Environment. 2015 Jan 22;4(1):24–36.

69. Güngördü A. Comparative toxicity of methidathion and glyphosate on early life stages of three amphibian species: Pelophylax ridibundus, Pseudepidalea viridis, and Xenopus laevis. Aquatic Toxicology. 2013 Sep 15;140–141:220–8.

70. El-Shenawy NS. Oxidative stress responses of rats exposed to Roundup and its active ingredient glyphosate. Environmental Toxicology and Pharmacology. 2009 Nov 1;28(3):379–85.

71. Uren Webster TM, Santos EM. Global transcriptomic profiling demonstrates induction of oxidative stress and of compensatory cellular stress responses in brown trout exposed to glyphosate and Roundup. BMC Genomics. 2015 Jan 31;16(1):32.

72. Nwani CD, Nagpure NS, Kumar R, Kushwaha B, Lakra WS. DNA damage and oxidative stress modulatory effects of glyphosate-based herbicide in freshwater fish, Channa punctatus. Environmental Toxicology and Pharmacology. 2013 Sep 1;36(2):539–47.

73. de Aguiar LM, Figueira FH, Gottschalk MS, da Rosa CE. Glyphosate-based herbicide exposure causes antioxidant defence responses in the fruit fly Drosophila melanogaster. Comparative Biochemistry and Physiology Part C: Toxicology & Pharmacology. 2016 Jul 1;185–186:94–101.

74. Puértolas L, Damásio J, Barata C, Soares AMVM, Prat N. Evaluation of side-effects of glyphosate mediated control of giant reed (Arundo donax) on the structure and function of a nearby Mediterranean river ecosystem. Environmental Research. 2010 Aug 1;110(6):556–64.

75. Kwiatkowska M, Nowacka-Krukowska H, Bukowska B. The effect of glyphosate, its metabolites and impurities on erythrocyte acetylcholinesterase activity. Environmental Toxicology and Pharmacology. 2014 May 1;37(3):1101–8.

76. Kwiatkowska M, Huras B, Bukowska B. The effect of metabolites and impurities of glyphosate on human erythrocytes (in vitro). Pesticide Biochemistry and Physiology. 2014 Feb 1;109:34–43.

77. González-Santoyo I, Córdoba-Aguilar A. Phenoloxidase: a key component of the insect immune system. Entomologia Experimentalis et Applicata. 2012;142(1):1–16.

78. Mylonakis E, Moreno R, Khoury JBE, Idnurm A, Heitman J, Calderwood SB, et al. Galleria mellonella as a Model System To Study Cryptococcus neoformans Pathogenesis. Infection and Immunity. 2005 Jul 1;73(7):3842–50.

79. Smith RC, Vega-Rodríguez J, Jacobs-Lorena M, Smith RC, Vega-Rodríguez J, Jacobs-Lorena M. The Plasmodium bottleneck: malaria parasite losses in the mosquito vector. Memórias do Instituto Oswaldo Cruz. 2014 Aug;109(5):644–61.

80. Sinden RE, Billingsley PF. Plasmodium invasion of mosquito cells: hawk or dove? Trends Parasitol. 2001 May;17(5):209–12.

81. Whitten MMA, Shiao SH, Levashina EA. Mosquito midguts and malaria: cell biology, compartmentalization and immunology. Parasite Immunology. 2006;28(4):121–30.

82. Gouagna LC, Gouagna LC, Mulder B, Mulder B, Noubissi E, Noubissi E, et al. The early sporogonic cycle of Plasmodium falciparum in laboratory-infected Anopheles gambiae: an estimation of parasite efficacy. Tropical Medicine & International Health. 1998;3(1):21–8.

1317 83. Dong Y, Manfredini F, Dimopoulos G. Implication of the Mosquito Midgut Microbiota in
1318 the Defense against Malaria Parasites. PLoS Pathog [Internet]. 2009 May 8 [cited
1319 2020 Apr 4];5(5). Available from:
1320 https://www.ncbi.nlm.nih.gov/pmc/articles/PMC2673032/

1321 84. Bahia AC, Dong Y, Blumberg BJ, Mlambo G, Tripathi A, BenMarzouk-Hidalgo OJ, et al.
1322 Exploring Anopheles gut bacteria for Plasmodium blocking activity. Environ
1323 Microbiol. 2014 Sep;16(9):2980–94.

1324 85. Bai L, Wang L, Vega-Rodríguez J, Wang G, Wang S. A Gut Symbiotic Bacterium Serratia
1325 marcescens Renders Mosquito Resistance to Plasmodium Infection Through
1326 Activation of Mosquito Immune Responses. Front Microbiol. 2019;10:1580.

1327 86. Romoli O, Gendrin M. The tripartite interactions between the mosquito, its microbiota
1328 and Plasmodium. Parasit Vectors. 2018 20;11(1):200.

1329 87. Mason HS. The chemistry of melanin; mechanism of the oxidation of
1330 dihydroxyphenylalanine by tyrosinase. J Biol Chem. 1948 Jan;172(1):83–99.

1331 88. Raper HS. The Tyrosinase-tyrosine Reaction. Biochem J. 1927;21(1):89–96.

1332 89. García-Borrón JC, Sánchez MCO. Biosynthesis of Melanins. In: Melanins and
1333 Melanosomes [Internet]. John Wiley & Sons, Ltd; 2011 [cited 2019 Jun 8]. p. 87–116.
1334 Available from:
1335 https://onlinelibrary.wiley.com/doi/abs/10.1002/9783527636150.ch4

1336 90. Jara JR, Solano F, Lozano JA. Assays for Mammalian Tyrosinase: A Comparative Study.
1337 Pigment Cell Research. 1988;1(5):332–9.

1338 91. Chen Q-X, Song K-K, Wang Q, Huang H. Inhibitory Effects on Mushroom Tyrosinase by
1339 Some Alkylbenzaldehydes. Journal of Enzyme Inhibition and Medicinal Chemistry.
1340 2003 Dec 1;18(6):491–6.

1341 92. Liu H-J, Ji S, Fan Y-Q, Yan L, Yang J-M, Zhou H-M, et al. The Effect of D-(−)-arabinose on
1342 Tyrosinase: An Integrated Study Using Computational Simulation and Inhibition
1343 Kinetics [Internet]. Vol. 2012, Enzyme Research. Hindawi; 2012 [cited 2020 Oct 27].
1344 p. e731427. Available from: https://www.hindawi.com/journals/er/2012/731427/

1345 93. Glass RL. Metal complex formation by glyphosate. J Agric Food Chem. 1984 Nov
1346 1;32(6):1249–53.

1347 94. Madsen HEL, Christensen HH, Gottlieb-Petersen C, Andresen AF, Smidsrød O, Pontchour
1348 C-O, et al. Stability Constants of Copper(II), Zinc, Manganese(II), Calcium, and
1349 Magnesium Complexes of N-(Phosphonomethyl)glycine (Glyphosate). Acta Chem
1350 Scand. 1978;32a:79–83.

95. Zhou C-F, Wang Y-J, Li C-C, Sun R-J, Yu Y-C, Zhou D-M. Subacute toxicity of copper and glyphosate and their interaction to earthworm (Eisenia fetida). Environmental Pollution. 2013 Sep 1;180:71–7.

96. Riley PA. Radicals in Melanin Biochemistry a. Annals of the New York Academy of Sciences. 1988;551(1):111–9.

97. Gordon MH. The Mechanism of Antioxidant Action in Vitro. In: Hudson BJF, editor. Food Antioxidants [Internet]. Dordrecht: Springer Netherlands; 1990 [cited 2019 Jun 8]. p. 1–18. (Elsevier Applied Food Science Series). Available from: https://doi.org/10.1007/978-94-009-0753-9_1

98. Choe E, Min DB. Mechanisms of Antioxidants in the Oxidation of Foods. Comprehensive Reviews in Food Science and Food Safety. 2009;8(4):345–58.

99. Jodko-Piórecka K, Litwinienko G. Antioxidant activity of dopamine and L-DOPA in lipid micelles and their cooperation with an analogue of α-tocopherol. Free Radical Biology and Medicine. 2015 Jun 1;83:1–11.

100. Bailey SI, Ritchie IM. A cyclic voltammetric study of the aqueous electrochemistry of some quinones. Electrochimica Acta. 1985 Jan 1;30(1):3–12.

101. Kissinger PT, Heineman WR. Cyclic voltammetry. J Chem Educ. 1983 Sep 1;60(9):702.

102. Liu X, Zhang Z, Cheng G, Dong S. Spectroelectrochemical and Voltammetric Studies of L-DOPA. Electroanalysis. 2003;15(2):103–7.

103. Fotouhi L, Tammari E, Asadi S, Heravi MM, Nematollahi D. Estimation of heterogeneous rate constants of reaction of electrochemically generated o-benzoquinones with various nucleophiles containing thiol group. International Journal of Chemical Kinetics. 2009 Jun 1;41(6):426–31.

104. Boyle JH, Dalgleish HJ, Puzey JR. Monarch butterfly and milkweed declines substantially predate the use of genetically modified crops. Proc Natl Acad Sci U S A. 2019 Feb 19;116(8):3006–11.

105. Wepprich T, Adrion JR, Ries L, Wiedmann J, Haddad NM. Butterfly abundance declines over 20 years of systematic monitoring in Ohio, USA. PLOS ONE. 2019 Jul 9;14(7):e0216270.

106. Wepprich T. Monarch butterfly trends are sensitive to unexamined changes in museum collections over time. PNAS. 2019 Jul 9;116(28):13742–4.

107. Thogmartin WE, Wiederholt R, Oberhauser K, Drum RG, Diffendorfer JE, Altizer S, et al. Monarch butterfly population decline in North America: identifying the threatening processes. Royal Society Open Science. 4(9):170760.

108. Molina-Cruz A, DeJong RJ, Ortega C, Haile A, Abban E, Rodrigues J, et al. Some strains of Plasmodium falciparum, a human malaria parasite, evade the complement-like system of Anopheles gambiae mosquitoes. PNAS. 2012 Jul 10;109(28):E1957–62.

109. Urabe K, Aroca P, Tsukamoto K, Mascagna D, Palumbo A, Prota G, et al. The inherent cytotoxicity of melanin precursors: A revision. Biochimica et Biophysica Acta (BBA) - Molecular Cell Research. 1994 Apr 28;1221(3):272–8.

110. Smith RC, Barillas-Mury C. Plasmodium Oocysts: Overlooked Targets of Mosquito Immunity. Trends Parasitol. 2016;32(12):979–90.

111. Hogg JC, Hurd H. The effects of natural Plasmodium falciparum infection on the fecundity and mortality of Anopheles gambiae s. l. in north east Tanzania. Parasitology. 1997 Apr;114 (Pt 4):325–31.

112. Okech BA, Gouagna LC, Kabiru EW, Beier JC, Yan G, Githure JI. Influence of age and previous diet of Anopheles gambiae on the infectivity of natural Plasmodium falciparum gametocytes from human volunteers. J Insect Sci [Internet]. 2004 Oct 22 [cited 2020 Oct 26];4. Available from: https://www.ncbi.nlm.nih.gov/pmc/articles/PMC1081565/

113. Bando H, Okado K, Guelbeogo WM, Badolo A, Aonuma H, Nelson B, et al. Intra-specific diversity of Serratia marcescens in Anopheles mosquito midgut defines Plasmodium transmission capacity. Scientific Reports. 2013 Apr 10;3(1):1–9.

114. Cirimotich CM, Dong Y, Clayton AM, Sandiford SL, Souza-Neto JA, Mulenga M, et al. Natural Microbe-Mediated Refractoriness to Plasmodium Infection in Anopheles gambiae. Science. 2011 May 13;332(6031):855–8.

115. Zhao H, Li G, Guo D, Wang Y, Liu Q, Gao Z, et al. Transcriptomic and metabolomic landscape of the molecular effects of glyphosate commercial formulation on Apis mellifera ligustica and Apis cerana cerana. Science of The Total Environment. 2020 Nov 20;744:140819.

116. Benoit JB, Vigneron A, Broderick NA, Wu Y, Sun JS, Carlson JR, et al. Symbiont-induced odorant binding proteins mediate insect host hematopoiesis. eLife [Internet]. 2017 [cited 2021 Feb 7];6. Available from: https://www.ncbi.nlm.nih.gov/pmc/articles/PMC5231409/

117. Dzhavakhiya V, Voinova TM, Popletaeva S, Statsyuk N, Mikityuk O, Nazarova TA, et al. Some natural and synthetic compounds inhibiting the biosynthesis of aflatoxin B1 and melanin in Aspergillus flavus. SEL'SKOKHOZYAISTVENNAYA BIOLOGIA. 2016 Sep 1;51:533–42.

118. Yu RJ, Scott EJV. N-(phosphonoalkyl)-amino acids, derivatives thereof and compositions and methods of use [Internet]. US7429575B2, 2008 [cited 2018 Jun 19]. Available from:

https://patents.google.com/patent/US7429575B2/en?q=melanin&q=aminophosphonic+acid&q=A61Q19%2f02

119. Seguin M-C, Babizhayev MA. Cosmetic composition useful notably for the skin whitening and melanogenesis inhibiting agent containing such a cosmetic composition [Internet]. US6280715B1, 2001 [cited 2018 Jun 19]. Available from: https://patents.google.com/patent/US6280715B1/en

120. Jiang N, Sun N, Xiao D, Pan J, Wang Y, Zhu X. A copper-responsive factor gene CUF1 is required for copper induction of laccase in Cryptococcus neoformans. FEMS Microbiol Lett. 2009 Jul 1;296(1):84–90.

121. Nenadis N, Wang L-F, Tsimidou M, Zhang H-Y. Estimation of Scavenging Activity of Phenolic Compounds Using the ABTS•+ Assay. J Agric Food Chem. 2004 Jul 1;52(15):4669–74.

122. Yu RJ, Scott EJV. Alpha hydroxyacids, alpha ketoacids and their use in treating skin conditions [Internet]. US4363815A, 1982 [cited 2019 Jun 8]. Available from: https://patents.google.com/patent/US4363815A/en

123. Brauman KA, Flörke M, Mueller ND, Foley JA. Widespread Occurrence of Glyphosate and its Degradation Product (AMPA) in U.S. Soils, Surface Water, Groundwater, and Precipitation, 2001-2009. AGU Fall Meeting Abstracts. 2011 Dec 1;44:H44A-08.

124. Hallmann CA, Sorg M, Jongejans E, Siepel H, Hofland N, Schwan H, et al. More than 75 percent decline over 27 years in total flying insect biomass in protected areas. PLoS ONE. 2017;12(10):e0185809.

125. Jarvis B. The Insect Apocalypse Is Here. The New York Times [Internet]. 2018 Nov 27 [cited 2020 May 6]; Available from: https://www.nytimes.com/2018/11/27/magazine/insect-apocalypse.html

126. Montgomery GA, Dunn RR, Fox R, Jongejans E, Leather SR, Saunders ME, et al. Is the insect apocalypse upon us? How to find out. Biological Conservation. 2020 Jan 1;241:108327.

127. Cardoso P, Leather SR. Predicting a global insect apocalypse. Insect Conservation and Diversity. 2019;12(4):263–7.

128. Saunders ME, Janes JK, O'Hanlon JC. Moving On from the Insect Apocalypse Narrative: Engaging with Evidence-Based Insect Conservation. BioScience. 2020 Jan 1;70(1):80–9.

129. Rosenheim JA, Ward PS. Insect diversity over 36 years at a protected Sierra Nevada (California) site: towards an evaluation of the insect apocalypse hypothesis. Ecological Entomology [Internet]. [cited 2020 Oct 25];n/a(n/a). Available from: https://onlinelibrary.wiley.com/doi/abs/10.1111/een.12888

130. Saunders ME. Ups and downs of insect populations. Nature Ecology & Evolution. 2019 Dec;3(12):1616–7.

131. Cornet S, Gandon S, Rivero A. Patterns of phenoloxidase activity in insecticide resistant and susceptible mosquitoes differ between laboratory-selected and wild-caught individuals. Parasites Vectors. 2013 Oct 31;6(1):315.

132. Rodrigues J, Brayner FA, Alves LC, Dixit R, Barillas-Mury C. Hemocyte Differentiation Mediates Innate Immune Memory in Anopheles gambiae Mosquitoes. Science. 2010 Sep 10;329(5997):1353–5.

133. Schindelin J, Arganda-Carreras I, Frise E, Kaynig V, Longair M, Pietzsch T, et al. Fiji: an open-source platform for biological-image analysis. Nature Methods. 2012 Jul;9(7):676–82.

134. Thompson PG, Smouse PE, Scofield DG, Sork VL. What seeds tell us about birds: a multi-year analysis of acorn woodpecker foraging movements. Movement Ecology. 2014 Jun 23;2(1):12.

135. Cornet S, Gandon S, Rivero A. Patterns of phenoloxidase activity in insecticide resistant and susceptible mosquitoes differ between laboratory-selected and wild-caught individuals. Parasites & Vectors. 2013 Oct 31;6(1):315.

136. Schloss PD, Westcott SL, Ryabin T, Hall JR, Hartmann M, Hollister EB, et al. Introducing mothur: Open-Source, Platform-Independent, Community-Supported Software for Describing and Comparing Microbial Communities. Appl Environ Microbiol. 2009 Dec 1;75(23):7537–41.

137. Chong J, Liu P, Zhou G, Xia J. Using MicrobiomeAnalyst for comprehensive statistical, functional, and meta-analysis of microbiome data. Nature Protocols. 2020 Mar;15(3):799–821.

138. Dhariwal A, Chong J, Habib S, King IL, Agellon LB, Xia J. MicrobiomeAnalyst: a web-based tool for comprehensive statistical, visual and meta-analysis of microbiome data. Nucleic Acids Res. 2017 03;45(W1):W180–8.

139. Winder AJ, Harris H. New assays for the tyrosine hydroxylase and dopa oxidase activities of tyrosinase. Eur J Biochem. 1991 Jun 1;198(2):317–26.

140. Maurya DK, Devasagayam TPA. Antioxidant and prooxidant nature of hydroxycinnamic acid derivatives ferulic and caffeic acids. Food Chem Toxicol. 2010 Dec;48(12):3369–73.

141. Therneau TM. coxme: Mixed Effects Cox Models [Internet]. 2020 [cited 2021 Feb 7]. Available from: https://CRAN.R-project.org/package=coxme

Figure 1

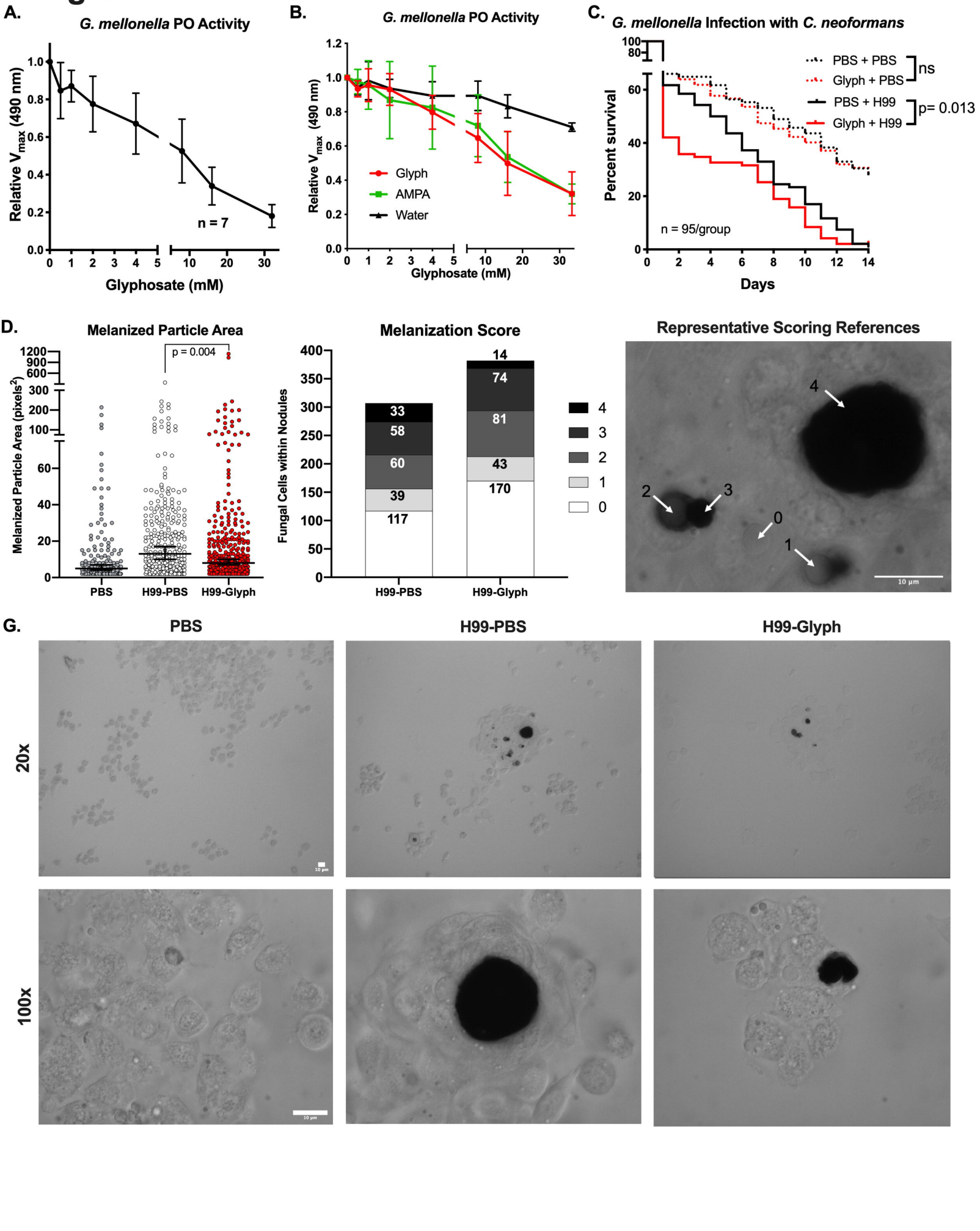

Figure 2

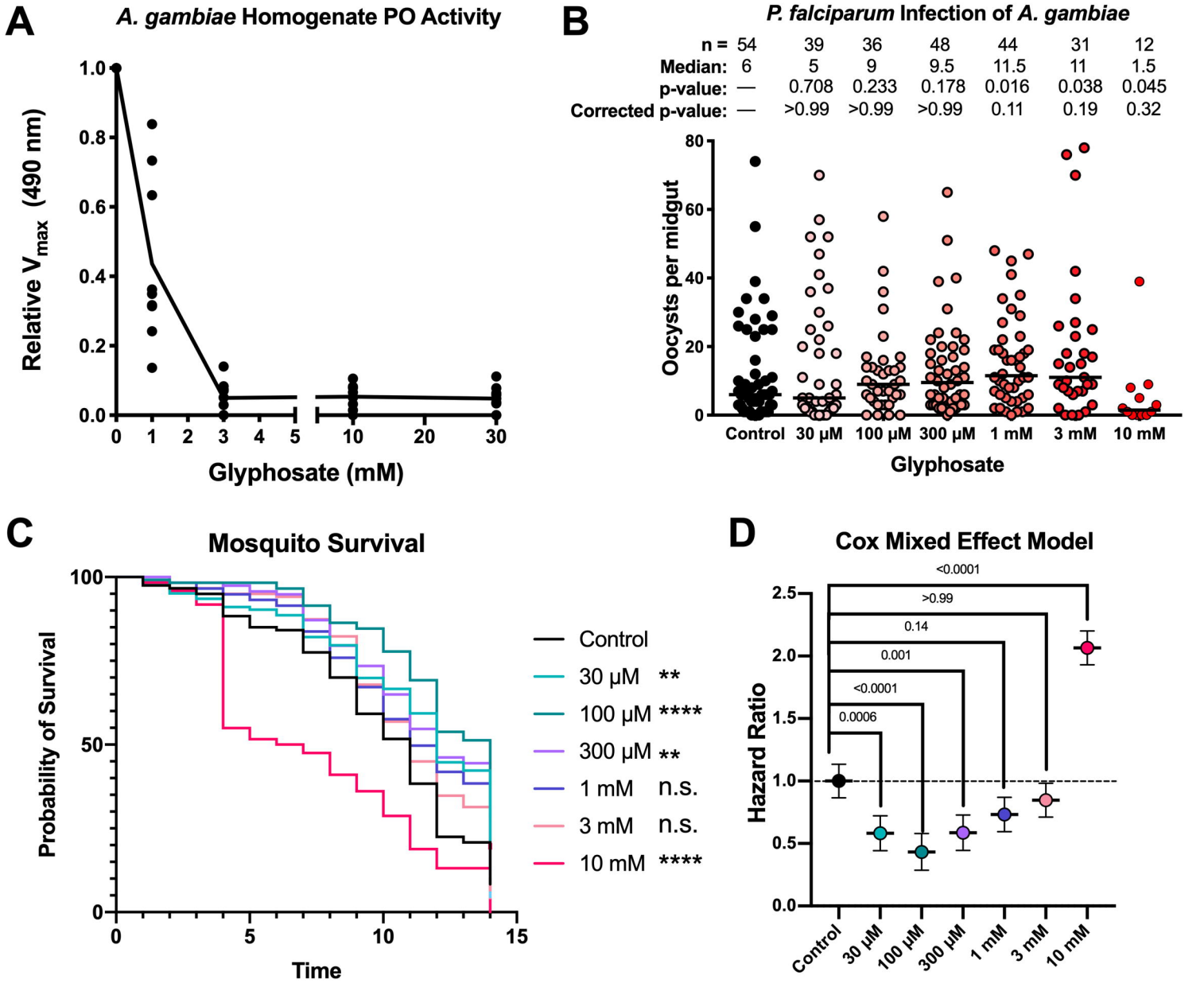
A
A. gambiae Homogenate PO Activity
Relative V_max (490 nm)
1.0
0.8
0.6
0.4
0.2
0.0
0 1 2 3 4 5 10 20 30
Glyphosate (mM)
B
P. falciparum Infection of A. gambiae
n = 54 39 36 48 44 31 12
Median: 6 5 9 9.5 11.5 11 1.5
p-value: — 0.708 0.233 0.178 0.016 0.038 0.045
Corrected p-value: — >0.99 >0.99 >0.99 0.11 0.19 0.32
Oocysts per midgut
80
60
40
20
0
Control 30 µM 100 µM 300 µM 1 mM 3 mM 10 mM
Glyphosate
C
Mosquito Survival
Probability of Survival
100
50
0
0 5 10 15
Time
Control
30 µM **
100 µM ****
300 µM **
1 mM n.s.
3 mM n.s.
10 mM ****
D
Cox Mixed Effect Model
Hazard Ratio
2.5
2.0
1.5
1.0
0.5
0.0
<0.0001
>0.99
0.14
0.001
<0.0001
0.0006
Control 30 µM 100 µM 300 µM 1 mM 3 mM 10 mM

Figure 3

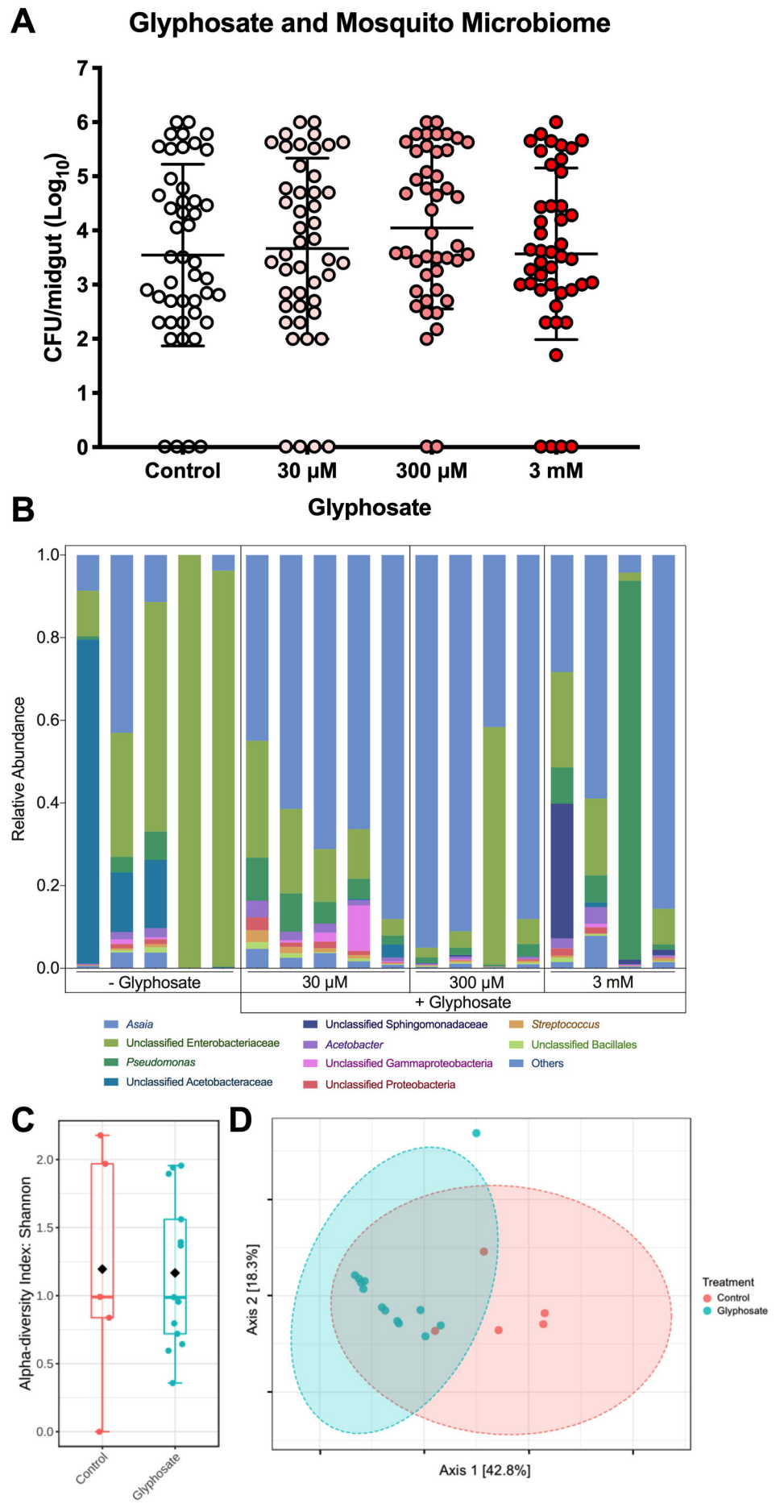
A
Glyphosate and Mosquito Microbiome
CFU/midgut (Log10)
0
1
2
3
4
5
6
7
Control
30 µM
300 µM
3 mM
Glyphosate
B
Relative Abundance
0.0
0.2
0.4
0.6
0.8
1.0
- Glyphosate
30 µM
300 µM
3 mM
+ Glyphosate
Asaia
Unclassified Enterobacteriaceae
Pseudomonas
Unclassified Acetobacteraceae
Unclassified Sphingomonadaceae
Acetobacter
Unclassified Gammaproteobacteria
Unclassified Proteobacteria
Streptococcus
Unclassified Bacillales
Others
C
Alpha-diversity Index: Shannon
0.0
0.5
1.0
1.5
2.0
Control
Glyphosate
D
Axis 2 [18.3%]
Axis 1 [42.8%]
Treatment
Control
Glyphosate

Figure 4

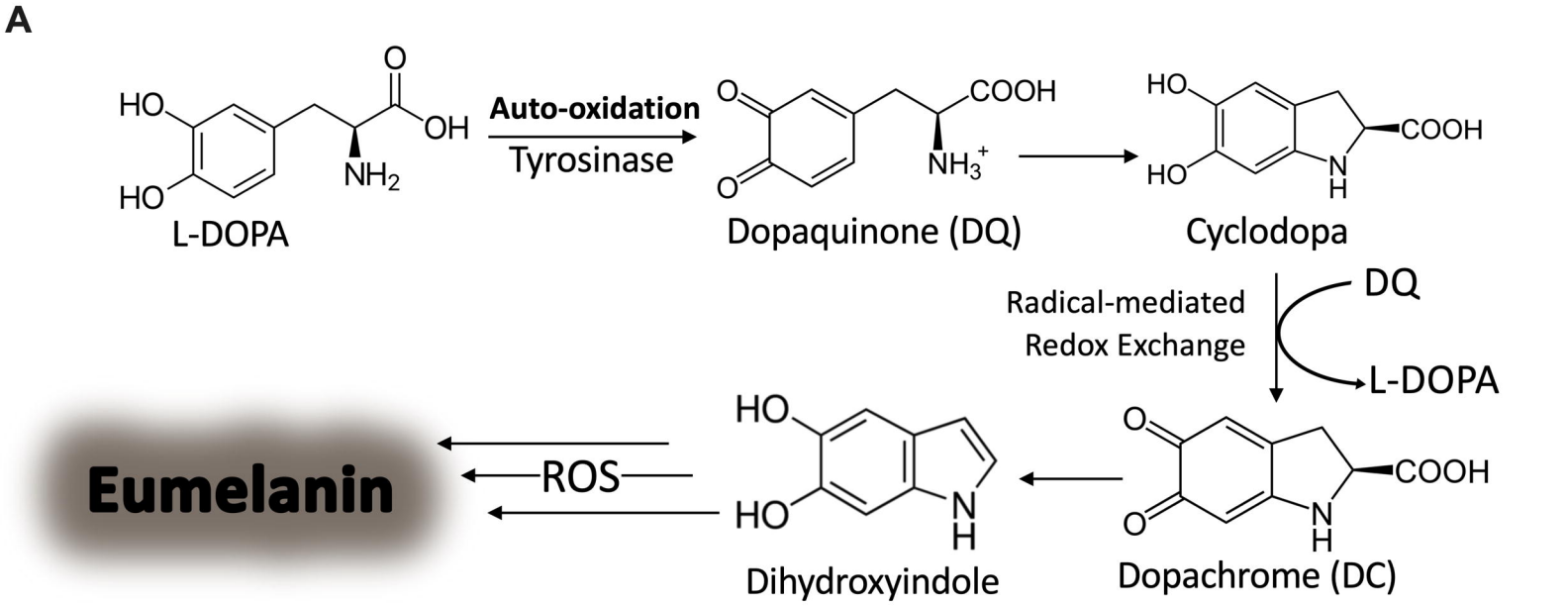
A
HO
HO
O
OH
NH2
L-DOPA
Auto-oxidation
Tyrosinase
O
O
COOH
NH3+
Dopaquinone (DQ)
HO
HO
COOH
N
H
Cyclodopa
Radical-mediated
Redox Exchange
DQ
L-DOPA
Eumelanin
ROS
HO
HO
N
H
Dihydroxyindole
O
O
COOH
N
H
Dopachrome (DC)

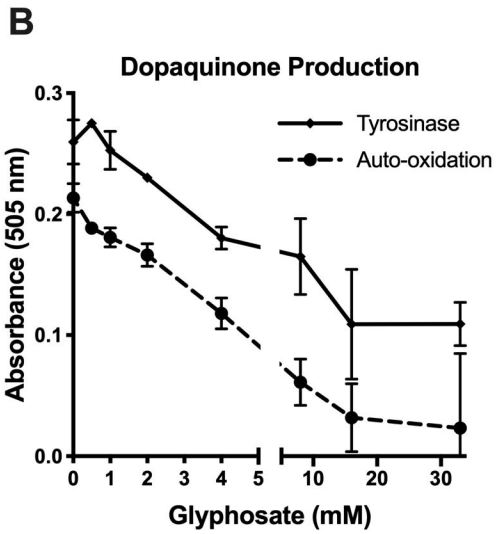
B
Dopaquinone Production
Tyrosinase
Auto-oxidation
Absorbance (505 nm)
0.3
0.2
0.1
0.0
0 1 2 3 4 5 10 20 30
Glyphosate (mM)

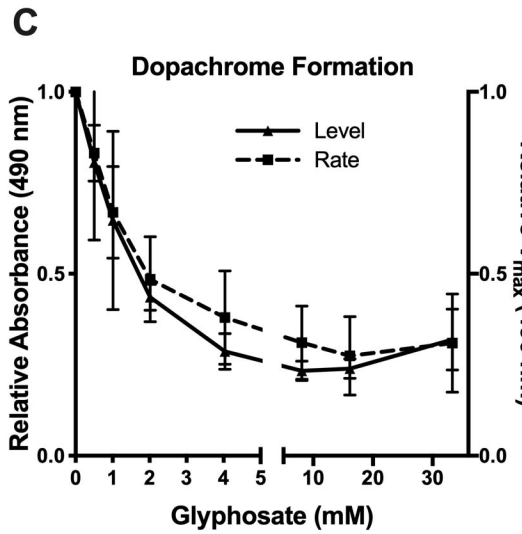
C
Dopachrome Formation
Level
Rate
Relative Absorbance (490 nm)
Relative Vmax (490 nm)
1.0
0.5
0.0
0 1 2 3 4 5 10 20 30
Glyphosate (mM)

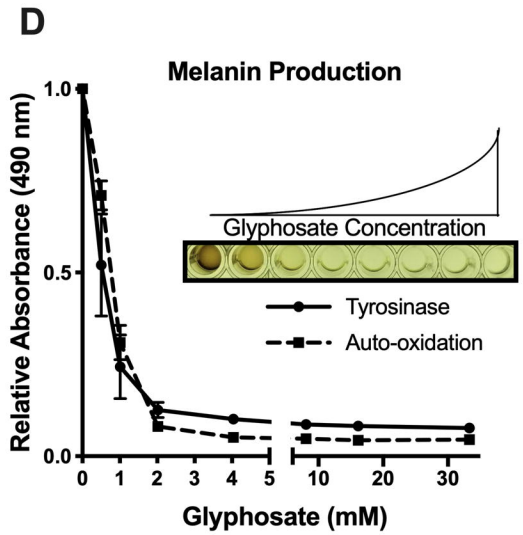
D
Melanin Production
Relative Absorbance (490 nm)
1.0
0.5
0.0
Glyphosate Concentration
Tyrosinase
Auto-oxidation
0 1 2 3 4 5 10 20 30
Glyphosate (mM)

Figure 5

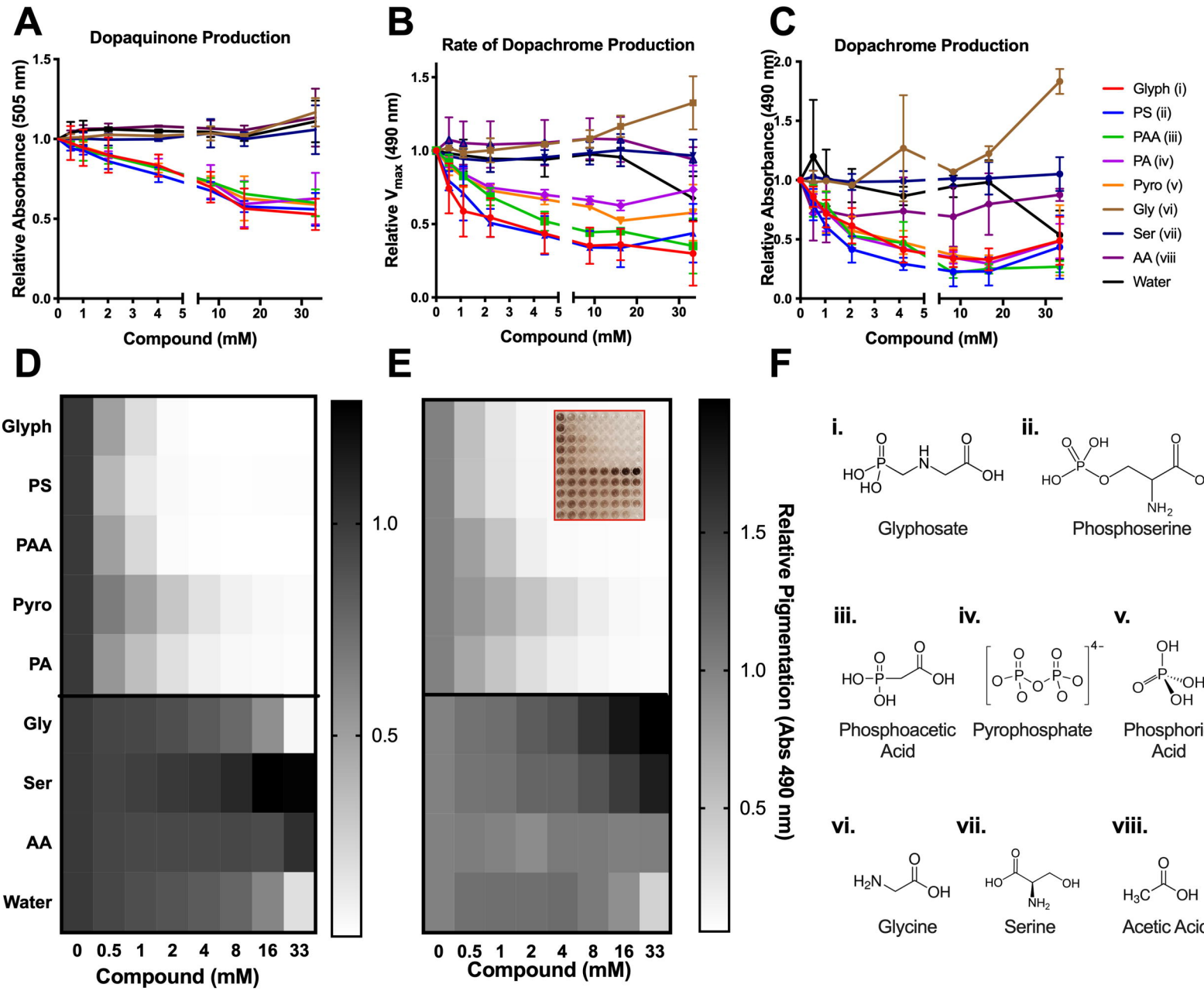
A
Dopaquinone Production
Relative Absorbance (505 nm)
Compound (mM)
B
Rate of Dopachrome Production
Relative V_{max} (490 nm)
Compound (mM)
C
Dopachrome Production
Relative Absorbance (490 nm)
Compound (mM)
Glyph (i)
PS (ii)
PAA (iii)
PA (iv)
Pyro (v)
Gly (vi)
Ser (vii)
AA (viii
Water
D
Glyph
PS
PAA
Pyro
PA
Gly
Ser
AA
Water
0 0.5 1 2 4 8 16 33
Compound (mM)
1.0
0.5
E
0 0.5 1 2 4 8 16 33
Compound (mM)
1.5
1.0
0.5
Relative Pigmentation (Abs 490 nm)
F
i.
Glyphosate
ii.
Phosphoserine
iii.
Phosphoacetic Acid
iv.
Pyrophosphate
v.
Phosphoric Acid
vi.
Glycine
vii.
Serine
viii.
Acetic Acid

Figure 6

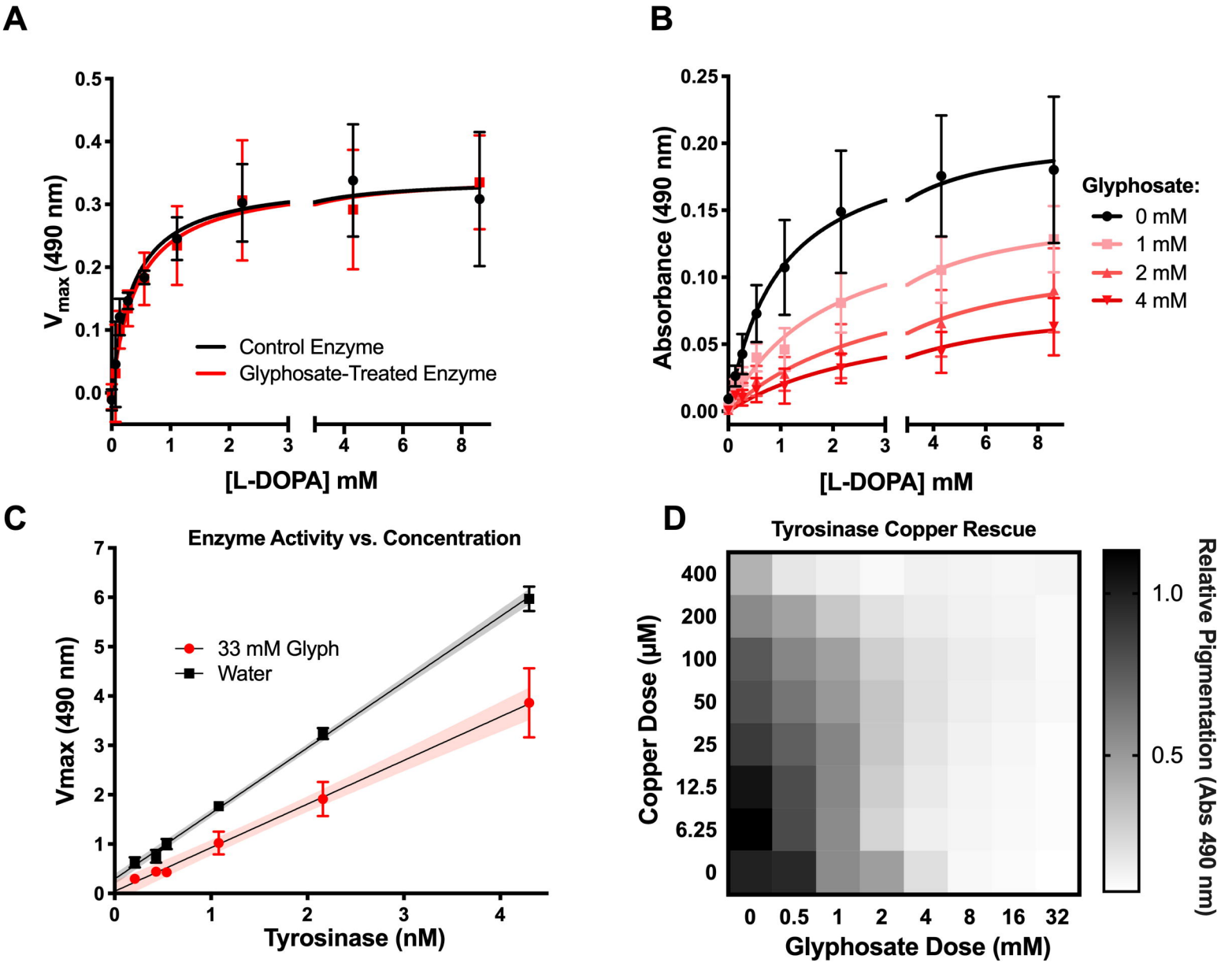
A
B
C
D
V_{max} (490 nm)
[L-DOPA] mM
Control Enzyme
Glyphosate-Treated Enzyme
Absorbance (490 nm)
Glyphosate:
0 mM
1 mM
2 mM
4 mM
Enzyme Activity vs. Concentration
Vmax (490 nm)
33 mM Glyph
Water
Tyrosinase (nM)
Tyrosinase Copper Rescue
Copper Dose (µM)
Glyphosate Dose (mM)
Relative Pigmentation (Abs 490 nm)

Figure 7

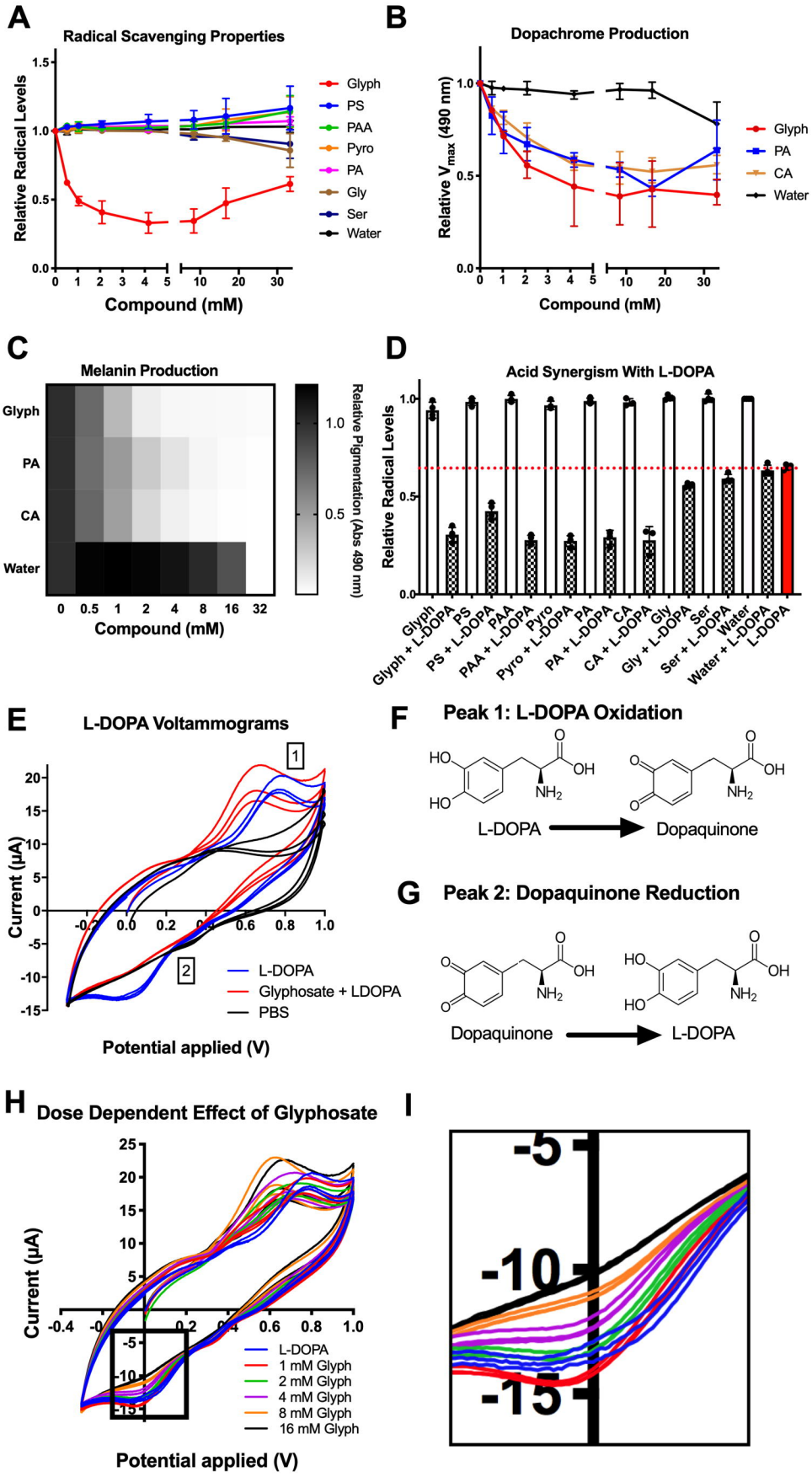
A
Radical Scavenging Properties
Relative Radical Levels
Compound (mM)
Glyph
PS
PAA
Pyro
PA
Gly
Ser
Water
B
Dopachrome Production
Relative V max (490 nm)
Compound (mM)
Glyph
PA
CA
Water
C
Melanin Production
Glyph
PA
CA
Water
Compound (mM)
Relative Pigmentation (Abs 490 nm)
D
Acid Synergism With L-DOPA
Relative Radical Levels
Glyph
Glyph + L-DOPA
PS
PS + L-DOPA
PAA
PAA + L-DOPA
Pyro
Pyro + L-DOPA
PA
PA + L-DOPA
CA
CA + L-DOPA
Gly
Gly + L-DOPA
Ser
Ser + L-DOPA
Water
Water + L-DOPA
L-DOPA
E
L-DOPA Voltammograms
Current (µA)
Potential applied (V)
L-DOPA
Glyphosate + LDOPA
PBS
F
Peak 1: L-DOPA Oxidation
L-DOPA
Dopaquinone
G
Peak 2: Dopaquinone Reduction
Dopaquinone
L-DOPA
H
Dose Dependent Effect of Glyphosate
Current (µA)
Potential applied (V)
L-DOPA
1 mM Glyph
2 mM Glyph
4 mM Glyph
8 mM Glyph
16 mM Glyph
I

Supplementary Figure 1

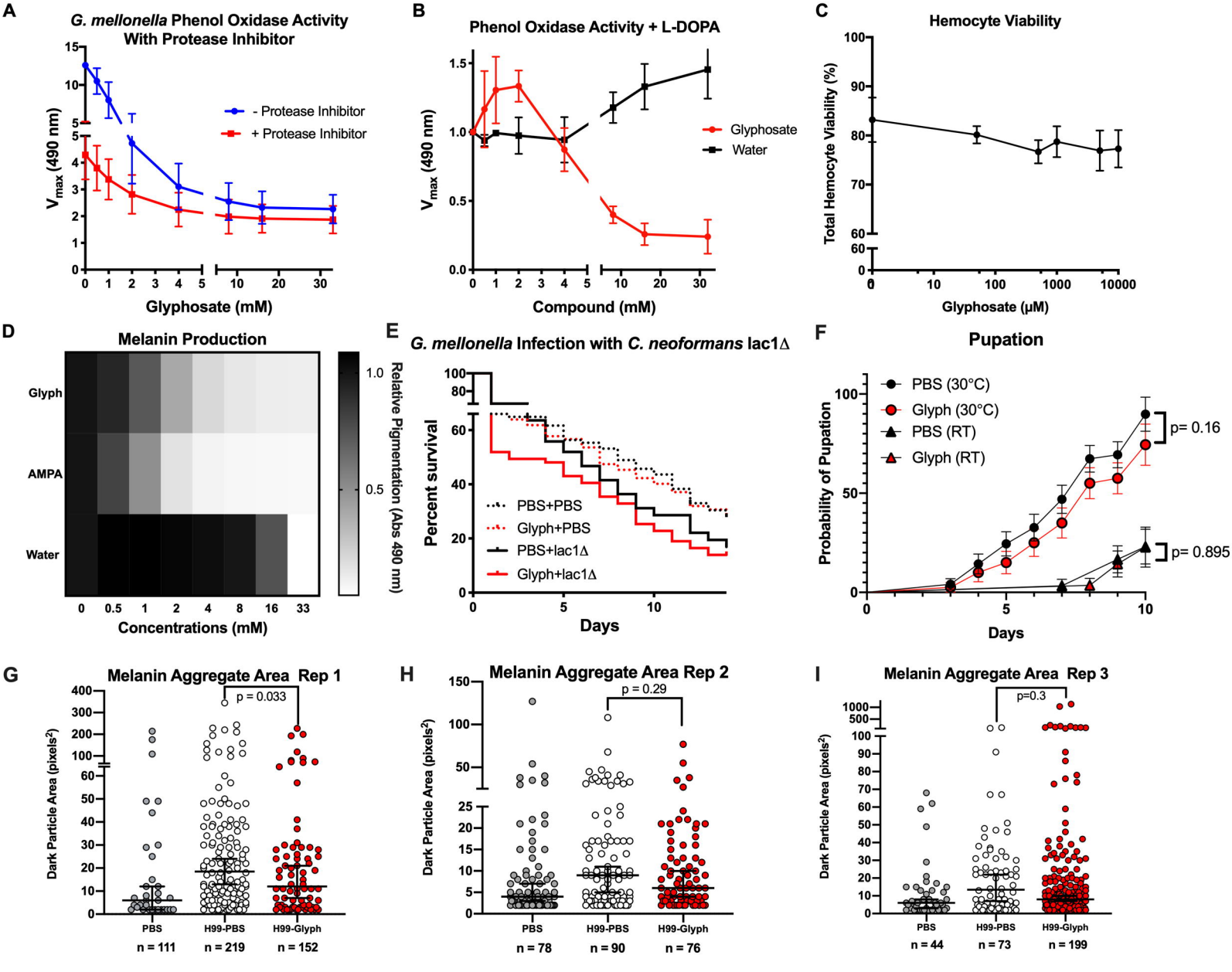

Supplementary Figure 2

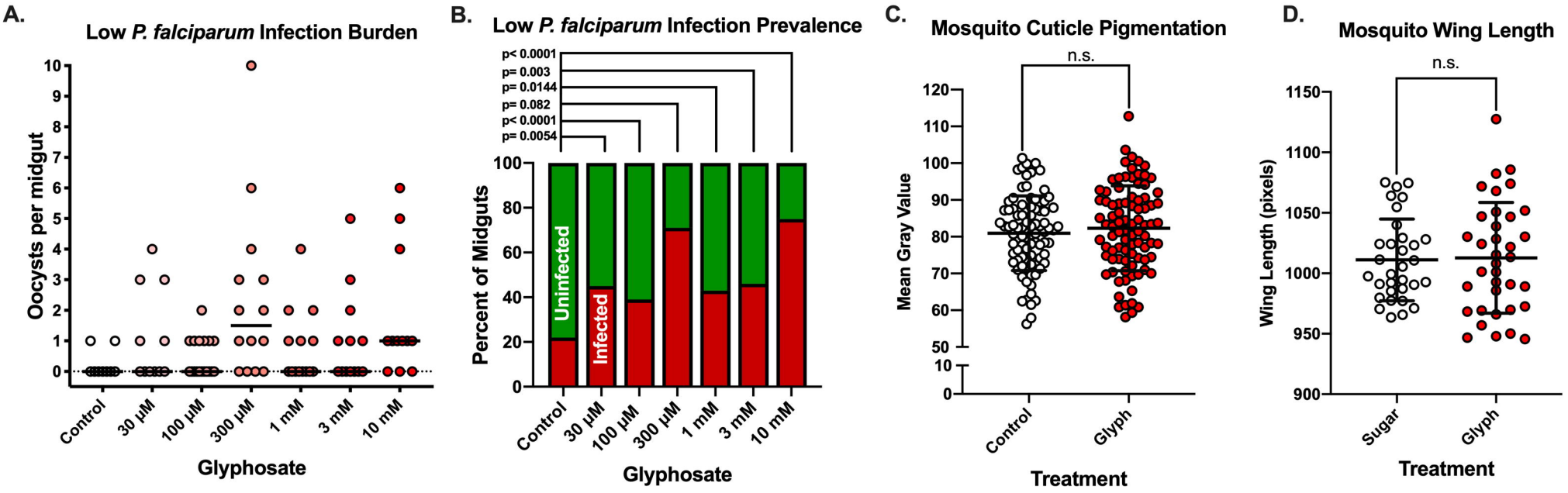

Supplementary Figure 3

A

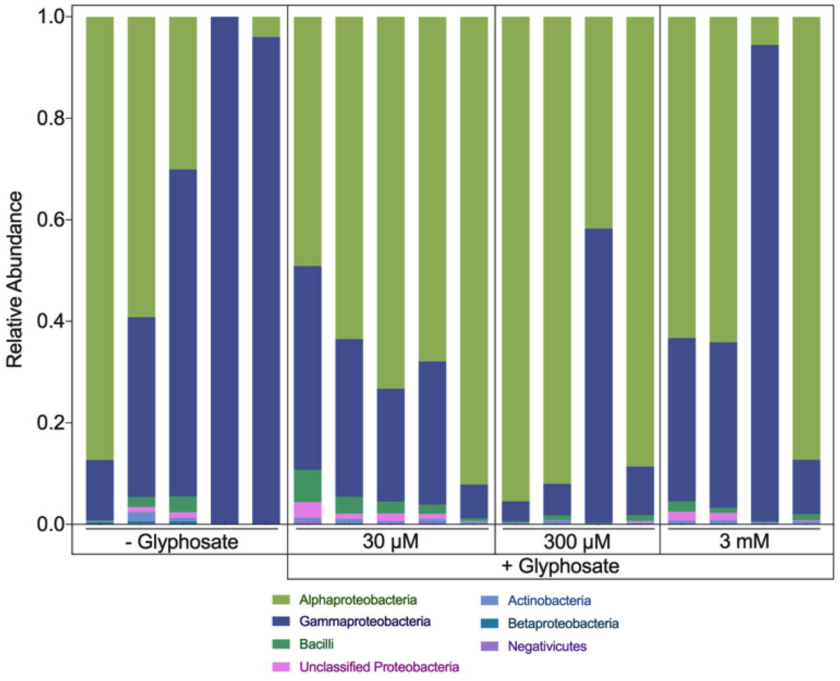

D

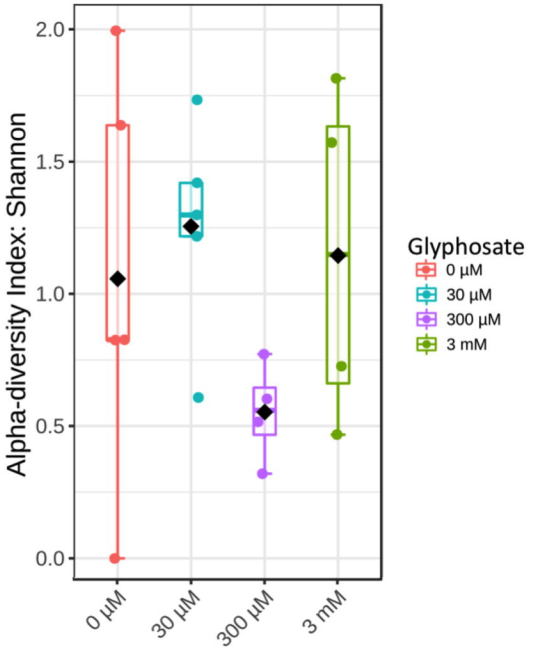

B

	[Glyphosate]			
Class	**- Glyphosate**	**30 µM**	**300 µM**	**3 mM**
Actinobacteria	0.0058	0.005642	0.002504	0.00476
Alphaproteobacteria	0.45129705	0.6918657	0.7944112	0.5505296
Bacilli	0.01333963	0.0286482	0.006664	0.0113333
Betaproteobacteria	0.0041215	0.000844	0.0001336	0.000471
Gammaproteobacteria	0.51917302	0.2566697	0.1942569	0.423504
Negativicutes	0.00042991	0.0025054	0.0003698	0.0005008
Unclassified Proteobacteria	0.00580703	0.013826	0.00166	0.0088853

C

	[Glyphosate]			
Genus	**- Glyphosate**	**30 µM**	**300 µM**	**3 mM**
Asaia	0.1336578	0.664002	0.789541	0.442692
Unclassified Enterobacteriaceae	0.58495882	0.155066	0.174655	0.130596
Pseudomonas	0.02301406	0.063686	0.01635	0.271084
Unclassified Acetobacteraceae	0.21889554	0.006761	0.000116	0.002701
Unclassified Sphingomonadaceae	0	0	0.001265	0.087311
Acetobacter	0.00847871	0.021091	0.003683	0.01762
Unclassified Gammaproteobacteria	0.00343976	0.028129	0.000996	0.00285
Unclassified Proteobacteria	0.00464562	0.013806	0.001663	0.008885
Streptococcus	0.00243342	0.013	0.002609	0.003708
Unclassified Bacillales	0.0039732	0.007579	0.00253	0.004348
Others	0.0164868	0.026856	0.006594	0.02819

E

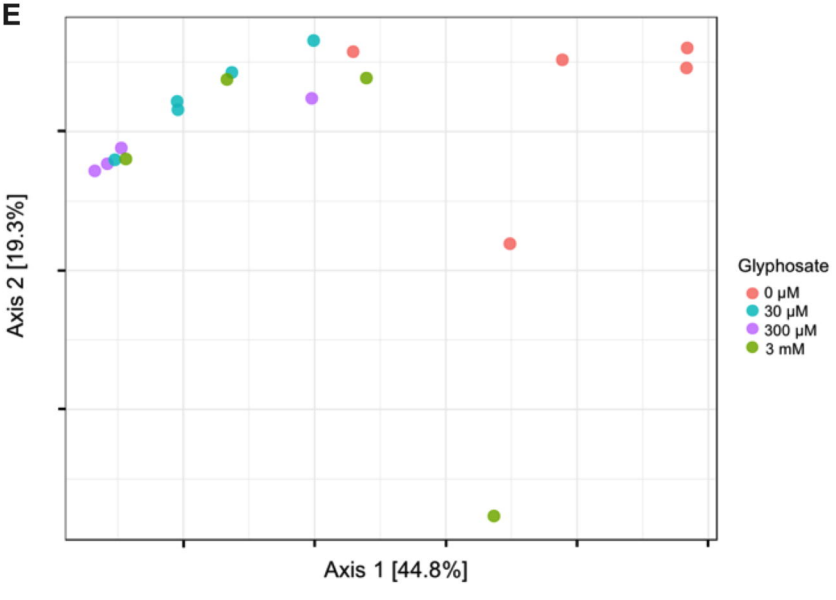

Supplementary Figure 4

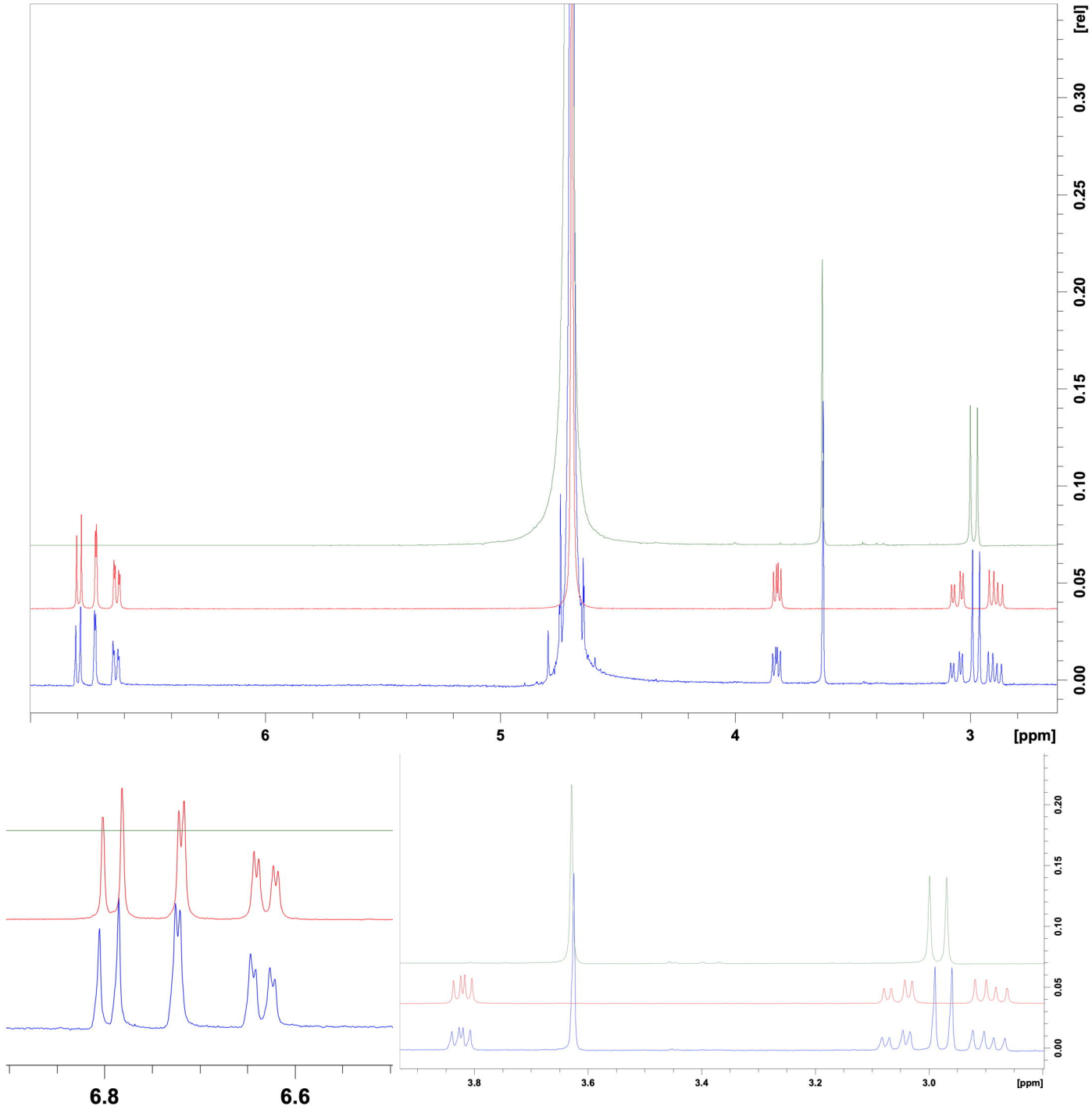

Supplementary Figure 5

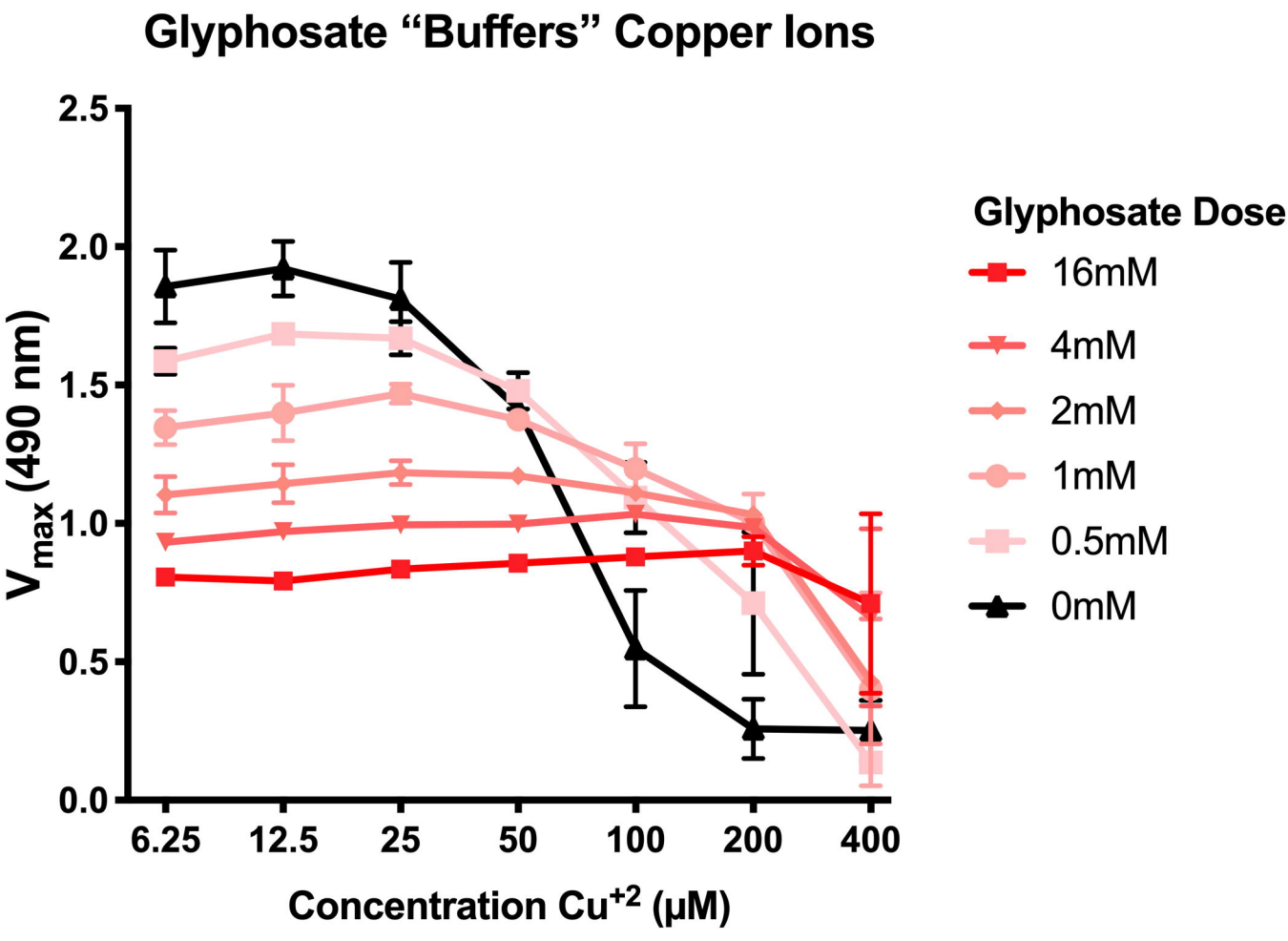

Supplementary Figure 6

A

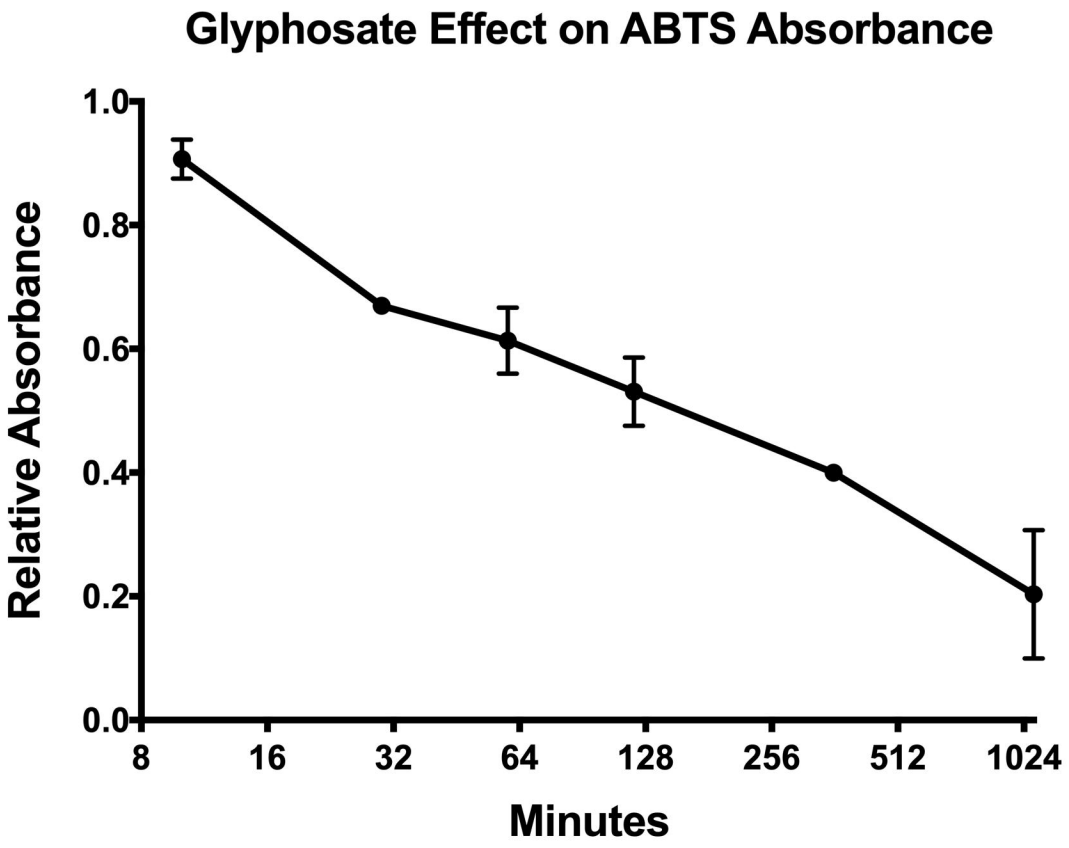

B

Compound	% Radical Quench-Compound Alone	% Radical Quench-Compound and L-DOPA	Synergy (Compared with L-DOPA alone)
Phosphoacetic Acid	0.020	72.288	0.483
Citric Acid	1.755	72.320	0.507
Phosphoric Acid	1.096	70.831	0.508
Pyrophosphate	3.320	72.675	0.526
Acetic Acid	1.327	64.155	0.565
Glyphosate	5.839	69.483	0.586
Phosphoserine	1.558	57.443	0.635
Glycine	-0.566	44.252	0.776
Serine	-0.386	40.808	0.846
Water	0.000	36.635	0.953
L-DOPA		**34.904**	**1.000**

Supplementary Figure 7

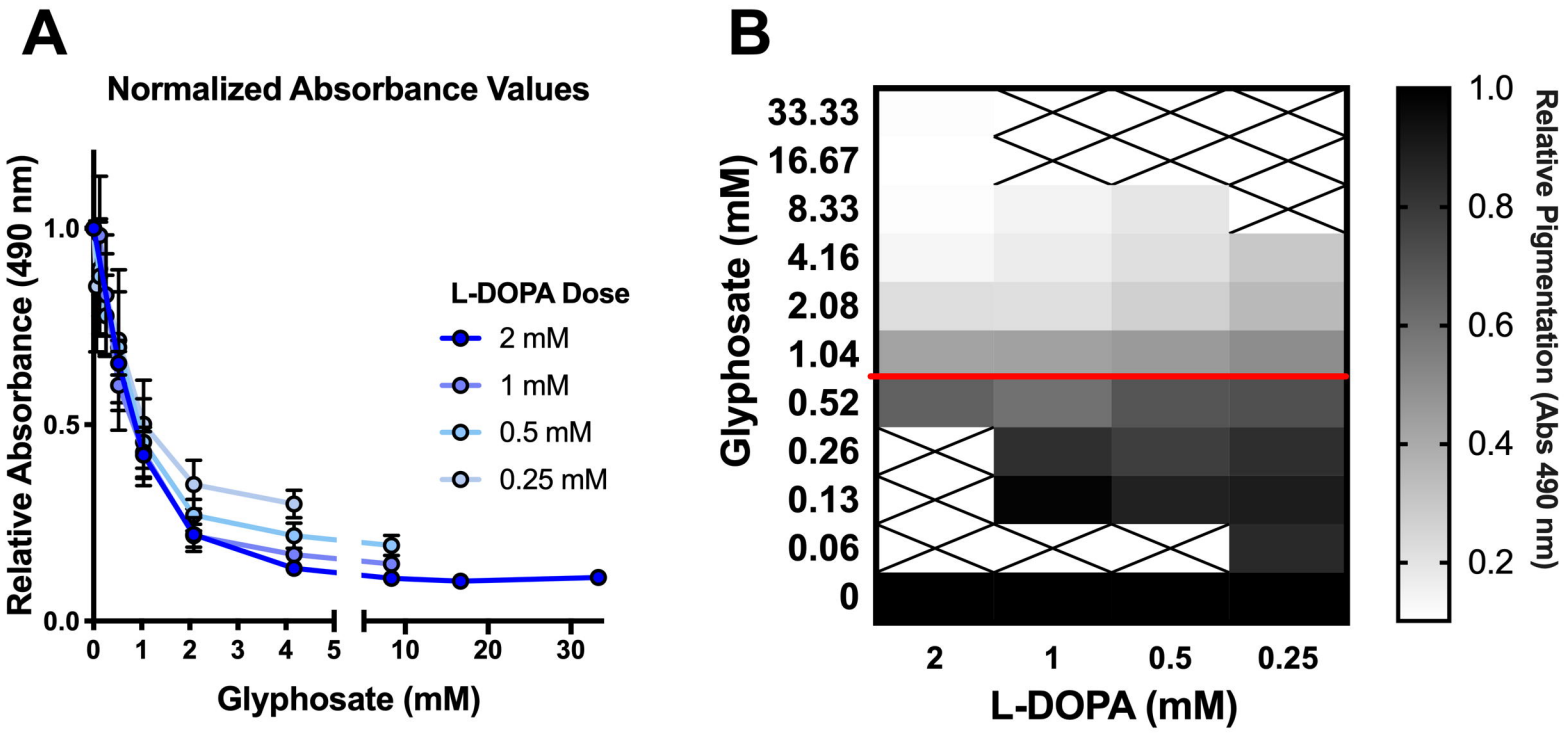

Supplementary Figure 8

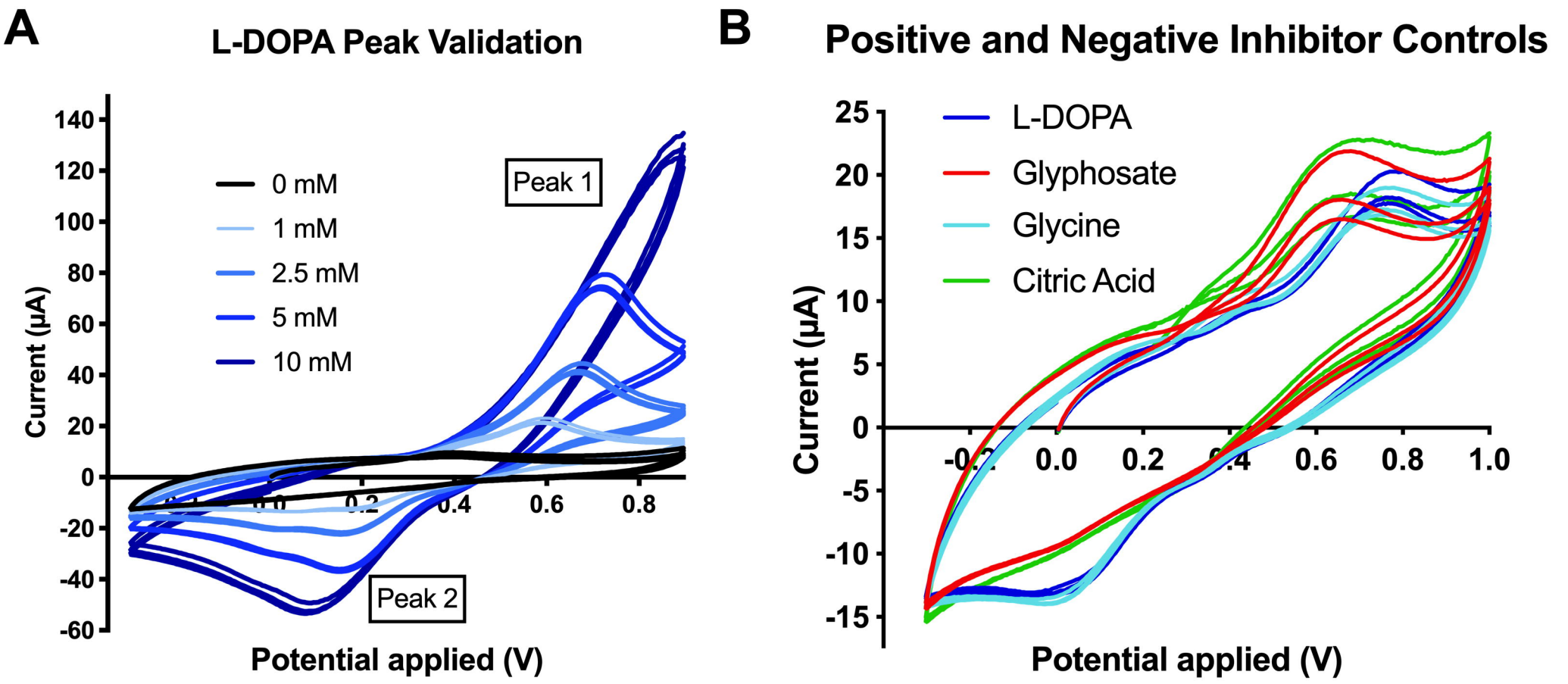

Supplementary Figure 9